NATIONAL ADVISORY COMMITTEE FOR AERONAUTICS

TECHNICAL NOTE 2511

CALCULATION OF HIGHER APPROXIMATIONS FOR TWO-DIMENSIONAL COMPRESSIBLE FLOW BY A SIMPLIFIED ITERATION PROCESS

By W. H. Braun and M. M. Klein

Lewis Flight Propulsion Laboratory
Cleveland, Ohio

NACA

Washington

October 1951

NATIONAL ADVISORY COMMITTEE FOR AERONAUTICS

TECHNICAL NOTE 2511

CALCULATION OF HIGHER APPROXIMATIONS FOR TWO-DIMENSIONAL COMPRESSIBLE FLOW BY A SIMPLIFIED ITERATION PROCESS

By W. H. Braun and M. M. Klein

SUMMARY

The iteration equations for a simplified solution of the nonlinear compressible-flow equation are developed and applied to two profiles, the ellipse and the Kaplan section. Limitations imposed on the solutions by simplifications in the differential equation and the boundary conditions are discussed. The velocities near the midchord, the critical and potential limit free-stream Mach numbers, and the extent of isentropic supersonic regions are calculated to four approximations for the Kaplan section and to six approximations for the ellipse. The development of the iteration equations and the presentation of the results are made in conformity with the Kármán transonic similarity law and comparisons are made with other solutions.

INTRODUCTION

Because of its nonlinear nature, the partial differential equation that describes the flow of a perfect compressible fluid has not yielded completely to any method of solution so far advanced. In fact, in such methods as the iteration procedures and the variational method (reference 1), it is not even attempted to find a closed-form solution or the general term of a series expansion; rather, a finite (and usually small) number of terms of a series expansion are obtained. Unfortunately, in such cases, whereas more and more terms are required as compressibility effects become more pronounced, the difficulty of securing the higher terms becomes inordinately greater. Although the difficulties of nonlinearity may be overcome by a transformation to the hodograph plane and the choice of a convenient gas law (reference 2), a new problem arises in the solution of any boundary-value problem because of the distortion of the boundary.

The solutions by iteration are begun by expanding the velocity potential as a series in terms of some flow parameter; it is then possible to determine each term from those which precede it by solving a

linear equation. Whenever the flow is over a thin body at relatively high speeds, it is preferable to expand the potential in terms of some parameter characteristic of the body, such as thickness ratio, camber coefficient, or angle of attack. The first term of the solution is a constant representing the undisturbed flow and the second is the well-known linearized or small perturbation compressible flow (Prandtl-Glauert solution). The procedure for obtaining successive terms is outlined by Ackeret (reference 3) and extended by Kaplan (reference 4), who applies it to a bump with no stagnation points and to a circular-arc profile. The higher-order terms were shown to be of greater consequence as the Mach number increased.

Recently Perl and Klein (reference 5) applied the Prandtl-Ackeret procedure, without specifying beforehand the parameter of expansion, to flows about thin bodies at transonic speeds. In their analysis, the flow equation is transformed to a new set of coordinates in which it is effectively expanded in powers of $\beta^2 = 1 - M_0^2$, where M_0 is the free-stream Mach number. In the transonic range $(\beta^2 \to 0)$, the lowest order terms in β^2 are dominant, and the transonic part of the flow equation is easily extracted.

The resulting transonic equation does not of itself preclude sizeable perturbations as long as β^2 is chosen sufficiently close to zero; however, the Perl-Klein process uses the customary small perturbation boundary condition, so that the solution of the complete problem - differential equation and boundary conditions - is termed the transonic limiting solution, limiting in the sense of Mach number near unity and geometric parameter near zero. This limiting nature of the solution is further emphasized by the form of the expansion parameter, which is found to be simply Kármán's transonic similarity parameter (reference 6), a quantity which combines the three definitive characteristics of the flow: the ratio of specific heats (that is, the type of gas), the free-stream Mach number, and the geometric parameter.

Although the iteration process greatly facilitates the solution of a nonlinear problem by substituting for it a series of linear problems, it, in turn, raises the difficult question of convergence of the series solution. The present analysis was made at the NACA Lewis laboratory to extend the calculations necessary to estimate the convergence of the iteration process of reference 6 where it is applied to two profiles, the ellipse and the Kaplan section. In particular, it will be found that the successive approximations suggest convergence not only of completely subsonic flows but also of some isentropic mixed flows.

There has been some dispute concerning the stability of the second type flow (see the résumé of these discussions by Sears, reference 7); one of the latest contributions is a stability investigation by Kuo

(reference 8), which indicates that decelerating transonic flows are unstable for a certain type disturbance. The result of the instability is the formation of a terminal shock in the supersonic region, with a consequent asymmetry. Some British measurements (references 9 and 10), however, indicate that small supersonic regions not terminated by shock waves may exist, or if shocks do occur, it is possible that they may not change the flow greatly from the isentropic pattern, provided that the free-stream Mach number is only slightly greater than critical. The isentropic mixed flows are therefore dealt with herein under the assumption that they are indicative of the nature of some real flows.

Another unpleasant feature of iteration methods, in addition to the question of convergence, is the large amount of labor involved. In obtaining the higher approximations by the present method, it is convenient to make certain simplifications in the differential equation so that the labor does not become too great. The justification for such changes and the limitations they impose on the solution will be discussed as they arise.

SMALL-PERTURBATION TRANSONIC FLOW

In reference 5 it is shown that the partial differential equation governing two-dimensional, irrotational, compressible flow may be written

$$(\beta^2\varphi_{xx} + \varphi_{yy})\left[1 - \frac{\gamma-1}{2} M_0^2 \left(2\varphi_x + \varphi_x^2 + \varphi_y^2\right)\right]$$

$$= \left[\Gamma_M \left(2\varphi_x + \varphi_x^2\right) + \frac{\gamma-1}{2} M_0^4 \varphi_y^2\right] \varphi_{xx} + M_0^2 \varphi_y^2 \varphi_{yy} + 2M_0^2 \left(1 + \varphi_x\right) \varphi_y \varphi_{xy} \tag{1}$$

where

$\beta^2 = 1 - M_0^2$

φ perturbation potential

γ ratio of specific heats of the gas

M_0 free-stream Mach number

$\Gamma_M = M_0^2 \left(1 + \frac{\gamma-1}{2} M_0^2\right)$

and the free-stream velocity has magnitude unity and the direction of positive x. (A complete list of symbols is given in the appendix.) If the flow is over an isolated body whose surface is defined by

$$y = \tau\, g(x)$$

where τ is the thickness ratio, the boundary conditions on the perturbation potential are

$$\left.\begin{aligned} \varphi_y &= \tau(1 + \varphi_x)\, g_x(x) \quad \text{at} \quad y = \tau\, g(x) \\ \varphi_x &= \varphi_y = 0 \qquad\qquad \text{at} \quad x^2 + y^2 = \infty \end{aligned}\right\} \tag{2}$$

For purposes of solution, it is desirable to write the second-order terms of equation (1) in normal form, as may be accomplished by the Prandtl-Glauert transformation. If the transformation is modified slightly, however, the coefficient of a nonlinear term of the same order in β^2 also becomes independent of flow parameters. The modified transformation is

$$\left.\begin{aligned} \bar{x} &= x \\ \eta &= \beta y \\ F(x,\eta) &= \frac{\Gamma_M}{\beta^2}\,\varphi(x,y) \end{aligned}\right\} \tag{3}$$

and it transforms the problem consisting of the differential equation (1) and the boundary conditions (2) into

$$\begin{aligned} (1 - 2F_x)F_{xx} + F_{\eta\eta} = {} & \beta^2\left((\gamma-1)\frac{M_0^2}{\Gamma_M}F_x\Delta F + \frac{1}{\Gamma_M}F_x{}^2F_{xx} + \frac{2M_0^2}{\Gamma_M}F_\eta F_{x\eta}\right) + \\ & \beta^4\left(\frac{\gamma-1}{2}\frac{M_0^2}{\Gamma_M^2}F_x{}^2\Delta F + \frac{\gamma-1}{2}\frac{M_0^4}{\Gamma_M^2}F_\eta{}^2F_{xx} + 2\,\frac{M_0^2}{\Gamma_M^2}F_xF_\eta F_{x\eta}\right) + \\ & \beta^6\left(\frac{\gamma-1}{2}\frac{M_0^2}{\Gamma_M^2}F_\eta{}^2\Delta F + \frac{M_0^2}{\Gamma_M^2}F_\eta{}^2F_{\eta\eta}\right) \end{aligned} \tag{4}$$

$$F_\eta = (1 + \varphi_x) \frac{\tau\Gamma_M}{\beta^3} g_x \quad \text{at} \quad \eta = \beta\tau g(x) \tag{5}$$

$$F_x = F_\eta = 0 \quad \text{at} \quad x^2 + \eta^2/\beta^2 = \infty \tag{6}$$

Figure 1 is the reciprocal of the transformation coefficient Γ_M/β^2 of equation (3).

A transition is now made to the small-perturbation transonic problem. For transonic speeds, the parameter β^2 approaches zero so that the right side of equation (4) may be neglected. Because of the nonlinearity of the right side, omission of these terms is especially justified if the perturbations are small. If the body considered is thin $(1 >> \tau)$ and there are no stagnation points, $\varphi_x << 1$ and the velocity φ_x may be neglected in boundary condition (5). For flows in which stagnation points occur, the effect of these stagnation points is assumed negligible in the region of interest in the flow field. Furthermore, in boundary condition (5), because the product β is a very small number and because (as will be shown) the solution for equation (7), which follows, has no singularities on the x-axis, it is assumed that the condition (that the velocity normal to the body is zero) may be made on the x-axis rather than on the body itself. This assumption is justified in reference 5. Consequently, the small-perturbation transonic flow problem is defined by

$$(1 - 2F_x) F_{xx} + F_{\eta\eta} = 0 \tag{7}$$

$$F_\eta = \frac{\tau\Gamma_M}{\beta^3} g_x \qquad \eta = 0 \tag{8}$$

$$F_x = F_\eta = 0 \qquad x^2 + \eta^2/\beta^2 = \infty \tag{9}$$

For values of $F_x < \frac{1}{2}$, the flow equation (7) is elliptic and for $F_x > \frac{1}{2}$ it is hyperbolic. In figure 2 the parabolic value of the perturbation velocity, $\varphi_x = \frac{\beta^2}{2\Gamma_M}$ (or $F_x = \frac{1}{2}$), is compared with the excess of the critical velocity over free-stream velocity, that is, the perturbation velocity at which a flow becomes locally sonic, as calculated from the Bernoulli equation. For such values of M_0 for which the two curves substantially agree, the differential equation (7) may be expected to describe mixed flows properly. The agreement is acceptable in the range $0.9 \leq M_0 \leq 1.1$, which is approximately the range of accuracy which

would have been suggested by equation (4). It is also observed at this point that if the error in the boundary condition (8) is to be limited to 10 percent as compared with the exact boundary condition (5), it is necessary that $\varphi_x < \frac{1}{10}$. Thus an examination of both the differential equation and the boundary condition indicates that flows in the transonic domain will be described sufficiently accurately only if they lie in the interval $0 < |\varphi_x| < \frac{1}{10}$.

The flows to be solved herein will be limited to those about bodies which are symmetric about the x- and y-axes. A limitation to subsonic free-stream Mach numbers is also necessary in order that the transformation (8) does not become imaginary. The results of the present method for high subsonic speeds can be applied, however, to slightly supersonic free-stream flows for which the detached shock wave is far ahead of the body and the Mach number downstream of the shock is as much below unity as the Mach number upstream is above unity. In this sense, the analysis is applicable to the entire range of transonic velocities.

ITERATION PROCESS

For convenience in describing the body, a transformation is made to elliptic coordinates, one of which is cyclic and can indicate position around the circumference of the body. These coordinates are compared with cartesian coordinates in figure 3. The equations defining the transformation are

$$x = \cosh s \cos t \tag{10}$$

$$\eta = \sinh s \sin t \tag{11}$$

$$J\left(\frac{x,\eta}{s,t}\right) = \cosh^2 s - \cos^2 t = \sinh^2 s + \sin^2 t \tag{12}$$

where $J\left(\frac{x,\eta}{s,t}\right)$ is the Jacobian or functional determinant of the x,y-coordinates with respect to s and t. The reciprocal of the Jacobian of the transformation is plotted in figure 4 as a function of t for several values of s.

The first derivatives of the potential in the new system are

$$F_x = (\sinh s \cos t\, F_s - \cosh s \sin t\, F_t)J^{-1} \tag{13}$$

$$F_\eta = (\cosh s \sin t\, F_s + \sinh s \cos t\, F_t)J^{-1} \tag{14}$$

which become at the axis of the body

$$F_x = -\frac{1}{\sin t} F_t \tag{15}$$

$$F_\eta = \frac{1}{\sin t} F_s \tag{16}$$

Substitution of these into the boundary condition (8) yields

$$F_s = -\frac{\tau \Gamma_M}{\beta^3} g_t \qquad s = 0 \tag{17}$$

Boundary condition (9) becomes

$$F_s = F_t = 0 \qquad s = \infty \tag{18}$$

An exact transformation of the flow equation (7) would result in the inverse Jacobian appearing in the nonlinear term, and it would be necessary to expand it in a Fourier series before employing a method of solution involving the separation of variables. The process used herein would then require the solution of an infinite number of ordinary differential equations. In order to simplify the analysis and to reduce the computational work that would ordinarily accompany such an expansion, only its first or constant term is retained. That is, in the transformation of equation (7) to elliptic coordinates, the Jacobian is set equal to 1, which is the first term in its expansion about the point $s = 0$, $t = \pi/2$. Of course, this simplification will restrict the region in which the equation is valid. A further restriction on the size of the region of validity is made by restricting the calculations to velocities on or near the surface of the body; thus $s \approx 0$ in the differential equation.

If the relation

$$F_{xx} + F_{\eta\eta} = J^{-1} (F_{ss} + F_{tt})$$

and equations (13) and (14) for the derivatives of F_x and F_η are used, equation (7) with the approximations

$$J \approx 1$$

$$\sinh s \approx 0$$

and

$$\cosh s \approx 1$$

may be written

$$F_{ss} + F_{tt} = - 2 \sin^2 t \, F_t \frac{\partial}{\partial t} (\sin t \, F_t)$$

$$= - 2 \sin^3 t \, F_t F_{tt} - 2 \sin^2 t \cos t \, F_t F_t \qquad (19)$$

This equation is proposed for use as a description of the flow in a region about the origin whose boundary is set by the criteria $\left| J^{-1} - 1 \right| \leq 0.10$ and $s \leq 0.1$. Such a region in the $x\eta$-plane is shown in figure 5, where for comparison a 10-percent-thick (in the xy-plane) Kaplan section is included as a typical profile. The length of the rectangle is seen to be about 0.3 chord.

With the change in the region of validity of the differential equation, there must be a change in the boundary conditions to correspond to this region. The surface boundary condition (7) may be retained as is; therefore only the outer boundaries (dashed rectangle in fig. 5) of the region lack boundary conditions. As a substitute for conditions on these boundaries, the boundary condition (18) at infinity is taken as a guide to postulate that, in the restricted region, both F_s and F_t must decrease with increasing s. The favorable comparison with more complete solutions shows that this condition prescribing monotonic character of the potential derivatives is sufficient. These comparisons are made in subsequent sections.

The method of solution of the problem, as formulated by the differential equation (19), the boundary condition (17), and the condition of monotoneity in s, is to write the transformed potential F as an infinite series

$$F \equiv F^1 + F^2 + F^3 + \ldots \qquad (20)$$

where it is assumed that the succeeding terms become progressively smaller at such a rate as to insure convergence of F and its derivatives. Definition (20) is placed in the flow equation (19), which is then arranged as follows:

$$\left.\begin{array}{l} {}^{1}_{s}F_{ss} + {}^{1}_{s}F_{tt} \\ \\ {}^{2}_{s}F_{ss} + {}^{2}_{s}F_{tt} \\ \\ {}^{3}_{s}F_{ss} + {}^{3}_{s}F_{tt} \\ \vdots \\ {}^{n}_{s}F_{ss} + {}^{n}_{s}F_{tt} \\ \vdots \end{array}\right\} = \left\{\begin{array}{l} 0 \\ \\ -2\sin^3 t\ {}^{1}_{s}F_{t}{}^{1}_{s}F_{tt} - 2\sin^2 t\cos t\ {}^{1}_{s}F_{t}{}^{1}_{s}F_{t} \\ \\ -2\sin^3 t\left({}^{2}_{s}F_{t}{}^{1}_{s}F_{tt} + {}^{1}_{s}F_{t}{}^{2}_{s}F_{tt}\right) - 2\sin^2 t\cos t\ 2\,{}^{1}_{s}F_{t}{}^{2}_{s}F_{t} \\ \vdots \\ -2\sin^3 t\sum_{\nu=1}^{n-1}{}^{\nu}_{s}F_{t}{}^{n-\nu}_{s}F_{tt} - 2\sin^2 t\cos t\sum_{\nu=1}^{n-1}{}^{\nu}_{s}F_{t}{}^{n-\nu}_{s}F_{t} \\ \vdots \end{array}\right. \tag{21}$$

This arrangement indicates that the equation should be divided for purposes of iteration into a sequence of equations each corresponding to one line of equation (21). In this way all terms which have the same total superscript value are grouped together; this procedure will later be seen equivalent to separating out terms of the same order in the Kármán similarity parameter.

The boundary condition on the body is also divided in a particular way among the terms in the series solution. The first term ${}^{1}_{s}F$ makes the total contribution:

$${}^{1}_{s}F_{s} = -\frac{\tau\Gamma_M}{\beta^3}\,g_t \qquad s = 0 \tag{22}$$

whereas the boundary conditions for all other terms are homogeneous:

$${}^{n}_{s}F_{s} = 0 \qquad s = 0 \qquad n \geq 2 \tag{23}$$

The condition of monotoneity requires that all ${}^{n}_{s}F_{s}$ and ${}^{n}_{s}F_{t}$ are monotone decreasing in s.

FIRST APPROXIMATION, ${}^{1}_{s}F$

The first approximation differs from subsequent approximations in that it requires the solution of the homogeneous Laplace equation (first

line of equation (21)) with a nonhomogeneous boundary condition (22). Higher approximations involve the solution of nonhomogeneous, or Poisson, equations with homogeneous boundary conditions. For this reason and to obtain the necessary start in the iteration procedure, the first approximation is treated separately.

The solution of this first iteration, which takes account of the monotoneity of the derivatives and of t as the cyclic coordinate, is

$$\overset{1}{F} = \sum_{k=1}^{\infty} e^{-ks} (\sigma_k \cos kt + \omega_k \sin kt) \tag{24}$$

Before this form is introduced into the boundary condition (22), the function $g(0,t)$ is expanded into a Fourier series and written

$$g(0,t) = \sum_{j} \delta_j \sin jt \tag{25}$$

In conformance with the restriction to bodies which are symmetric about the y-axis and about which there is no circulation, no cosine terms appear in the expansion. The index j is limited to odd values because of the symmetry of g about $t = \frac{\pi}{2}$. The introduction of expressions (24) and (25) into the boundary condition on the body (22) leads to

$$-\sum_{k=1}^{\infty} k(\sigma_k \cos kt + \omega_k \sin kt) = -\frac{\tau\Gamma_M}{\beta^3} \sum_{j=1}^{\infty} j\delta_j \cos jt \tag{26}$$

j odd only

It follows that

$$\overset{1}{F} = \frac{\tau\Gamma_M}{\beta^3} \sum_{k=1}^{\infty} \delta_k e^{-ks} \cos kt \tag{27}$$

k odd only

The nature of the dependence of $\overset{1}{F}$ on $\frac{\tau\Gamma_M}{\beta^3}$, a quantity combining the entire dependence of the first approximation on the parameters of the flow (reference 6), has the consequences immediately observed from equation (21) that

$$\left.\begin{aligned} {}^{2}F &\approx \left(\frac{\tau\Gamma_M}{\beta^3}\right)^2 \\ {}^{3}F &\approx \left(\frac{\tau\Gamma_M}{\beta^3}\right)^3 \\ &\cdot \quad\quad \cdot \\ &\cdot \quad\quad \cdot \\ {}^{n}F &\approx \left(\frac{\tau\Gamma_M}{\beta^3}\right)^n \end{aligned}\right\} \tag{28}$$

The quantity

$$K \equiv \frac{\tau\Gamma_M}{\beta^3}$$

is recognized as the similarity parameter of reference 5, and reduces to Kármán's similarity parameter (reference 6) as $M_0 \to 1$. Hence, as previously claimed, equation (21) is the ordering in powers of K with respect to this parameter. The similarity parameter is plotted as a function of M_0 for various τ in figure 6, which is reproduced from reference 5.

Writing ${}^{n}F \equiv {}^{n}f K^n$ gives the perturbation potential, by the transformation (3), as

$$\varphi = \frac{\tau}{\beta}\left({}^{1}f + {}^{2}fK + {}^{3}fK^2 + \cdots\right)$$

$$\equiv \frac{\tau}{\beta}\left[\left(\sum_{k=1}^{\infty} \delta_k e^{-ks}\cos kt\right) + f^2K + f^3K^2 + \cdots\right] \tag{29}$$

The first term inside the parenthesis represents an incompressible flow. Hence, for very small values of τ, for which K is also small, the transonic potential (29) reduces to the Prandtl-Glauert rule.

HIGHER APPROXIMATIONS

Inasmuch as all the ${}^{n}F$ beyond the first satisfy the same general form of differential equation and have the same boundary condition, it

is possible to treat the general form of F^n rather than each approximation separately. In the following discussion, an induction argument will be used to show that every term in the series for the transformed potential has the form

$$F^{\lambda} = K^{\lambda} \sum_{r=1}^{\lambda(\mu+3)-3} \sum_{p=1}^{\lambda(\mu+3)-3} (L^{\lambda}_{rp} + M^{\lambda}_{rp} s + N^{\lambda}_{rp} s^2 + \ldots) e^{-ps} \cos rt \qquad (30)$$

r odd only

where L^{λ}_{rp}, M^{λ}_{rp}, and N^{λ}_{rp} are constants and μ is the number of terms in the expansion (equation (25)) of $q(t)$, the function characterizing the shape of the body. The main part of the argument is to show that if equation (30) is true for all $\lambda < n$, then it is also true for $\lambda = n$.

From equation (21), the differential equation satisfied by any term F^n $(n > 1)$ is

$$F^n_{ss} + F^n_{tt} = -2 \sin^3 t \sum_{\nu=1}^{n-1} F^{\nu}_t F^{n-\nu}_{tt} - 2 \sin^2 t \cos t \sum_{\nu=1}^{n-1} F^{\nu}_t F^{n-\nu}_t \qquad (31)$$

Use of the postulated form (30) for F^{ν} and $F^{n-\nu}$ leads to the expansion for (31),

$$F_{ss}^{n} + F_{tt}^{n} = -\frac{K^n}{8} \sum_{\nu=1}^{n-1} \sum_{m=1}^{\nu(\mu+3)-3} \sum_{p=1}^{(n-\nu)(\mu+3)-3} \sum_{k=1}^{\nu(\mu+3)-3} \sum_{r=1}^{(n-\nu)(\mu+3)-3}$$

$$(L_{km}^{\nu} + sM_{km}^{\nu} + s^2N_{km}^{\nu} + \ldots)(L_{rp}^{n-\nu} + sM_{rp}^{n-\nu} + s^2N_{rp}^{n-\nu} + \ldots)$$

$$e^{-(p+m)s}\Big[(-3kr^2-kr)\cos(k+r+1)t + (-3kr^2+kr)\cos(k-r+1)t +$$

$$(3kr^2+kr)\cos(k-r-1)t + (3kr^2-kr)\cos(k+r-1)t +$$

$$(kr+kr^2)\cos(k+r+3)t + (kr-kr^2)\cos(k+r-3)t +$$

$$(-kr+kr^2)\cos(k-r+3)t + (-kr-kr^2)\cos(k-r-3)t\Big] \qquad (32)$$

k, r odd only

The right side of the foregoing equation is the sum of products involving the constants L_{km}^{ν}, M_{km}^{ν}, N_{km}^{ν}, . . ., powers of s, exponentials in s, and cosines of angles of multiple t. Accordingly, after all five summations have been accomplished and regroupings made according to powers of s, exponentials in s, and multiples of t, the equation will be

$$F_{ss}^{n} + F_{tt}^{n} = K^n \sum_{h=1}^{n(\mu+3)-3} \sum_{j=2}^{n(\mu+3)-6} (A_{hj}^{n} + sB_{hj}^{n} + s^2C_{hj}^{n} + \ldots)e^{-js}\cos ht \qquad (33)$$

h odd only

If a solution

$$F^{n} = K^n \sum_{h}^{n(\mu+3)-3} q_h^{n}(s)\cos ht \qquad (34)$$

h odd only

is assumed, the coefficient of each harmonic term in (33) must vanish. Thus

$$\frac{d^2}{ds^2}\overset{n}{q_h}(s) - h^2\overset{n}{q_h}(s) = \sum_{j=1}^{n(\mu+3)-6} (\overset{n}{A_{hj}} + s\overset{n}{B_{hj}} + s^2\overset{n}{C_{hj}} + \ldots)\, e^{-js} \tag{35}$$

h odd only

The particular integral of this equation is

$$\overset{n}{P_h} = \sum_{j\neq h} \overset{n}{A_{hj}} \frac{e^{-js}}{j^2-h^2} - \frac{\overset{n}{A_{hh}} s e^{-hs}}{2h} +$$

$$\sum_{j\neq h} \overset{n}{B_{hj}} \left[\frac{se^{-js}}{j^2-h^2} + \frac{2je^{-js}}{(j^2-h^2)^2}\right] - \overset{n}{B_{hh}} e^{-hs}\left(\frac{s^2}{4h} + \frac{s}{4h^2}\right) +$$

$$\sum_{j\neq h} \overset{n}{C_{hj}} \frac{e^{-js}}{j^2-h^2}\left[s^2 + \frac{4js}{j^2-h^2} + \frac{6j^2+2h^2}{(j^2-h^2)^2}\right] - \overset{n}{C_{hh}} e^{-hs}\left(\frac{s^3}{6h} + \frac{s^2}{4h^2} + \frac{s}{4h^3}\right) + \ldots \tag{36}$$

Here the notation $\sum_{j\neq h}$ refers to a summation over all values of j except $j = h$. The complementary function is $\overset{n}{G_h} e^{-hs}$, where $\overset{n}{G_h}$ may be found from the boundary condition on the body (23):

$$-h\overset{n}{G_h} + \left(\frac{d\overset{n}{P_h}}{ds}\right)_{s=0} = 0 \qquad n \geq 2 \tag{37}$$

Then

$$q_h^n = \frac{1}{h}\left(\frac{dP_h^n}{ds}\right)_{s=0} e^{-hs} + P_h^n$$

$$\equiv \sum_{j=1}^{n(\mu+3)-6} (I_{hj}^n + sM_{hj}^n + s^2N_{hj}^n + s^3O_{hj}^n + \ldots) e^{-js} \qquad (38)$$

where

$$L_{hj}^n = \sum_{j\neq h} \frac{1}{j^2-h^2}\left[A_{hj}^n + B_{hj}^n \frac{2j}{j^2-h^2} + C_{hj}^n \frac{6j^2+2h^2}{(j^2-h^2)^2} + \ldots\right]$$

$$L_{hh}^n = \sum_{j\neq h} \frac{1}{h(j^2-h^2)}\left\{-jA_{hj}^n + B_{hj}^n\left(1-\frac{2j^2}{j^2-h^2}\right) + C_{hj}^n\left[-j\frac{6j^2+2h^2}{(j^2-h^2)^2} + \frac{4j}{(j^2-h^2)}\right] + \ldots\right\} -$$

$$\left(A_{hh}^n \frac{1}{2h^2} + B_{hh}^n \frac{1}{4h^3} + C_{hh}^n \frac{1}{4h^4} + \ldots\right)$$

$$M_{hj}^n = \sum_{j\neq h} \frac{1}{j^2-h^2}\left(B_{hj}^n + \frac{4j}{j^2-h^2} C_{hj}^n + \ldots\right)$$

$$M_{hh}^n = -\left(A_{hh}^n \frac{1}{2h} + B_{hh}^n \frac{1}{4h^2} + C_{hh}^n \frac{1}{4h^2} + \ldots\right)$$

$$N_{hj}^n = \sum_{j\neq h} \frac{1}{j^2-h^2} C_{hj}^n + \ldots$$

$$N_{hh}^n = -\left(B_{hh}^n \frac{1}{4h} + C_{hh}^n \frac{1}{4h^2} + \ldots\right)$$

$$O_{hh}^n = -C_{hh}^n \frac{1}{6h} + \ldots \qquad (39)$$

(The maximum value of h for any n in equations (38) and (39) is $n(\mu+3)-3$.) Finally, if equation (38) is placed in the assumed form (34), the n^{th} approximation becomes

$$F^n = K^n \sum_{h=1}^{n(\mu+3)-3} \sum_{j=1}^{n(\mu+3)-3} \left(L_{hj}^n + sM_{hj}^n + s^2 N_{hj}^n + s^3 O_{hj}^n + \cdots \right) e^{-js} \cos ht \qquad (40)$$

h odd only

which is exactly the form postulated in equation (30).

It has been shown that if F^{ν} has the form (30) for all $\nu < n$, it will also have that form for $\nu = n$; there remains only to test this form on a particular approximation in order to complete the induction proof. If the second approximation is taken to correspond to the n^{th} approximation of the proposition, a comparison of all previous approximations (equation (27), in this case) indicates that the n^{th} (second) and, hence, all approximations subsequent to it must obey the form (30). The fact that the method of solution for the first approximations differs from that of subsequent approximations does not interfere with the argument.

The actual mechanics of the iteration process have been derived in the foregoing development and are outlined by equations (32), (33), (39), and (40). For example, after the first approximation has been obtained, the differential equation for the second may be found by setting $n = 2$ in equation (32) and letting k, r, m, and p assume values in accordance with the form of F^1. After all the coefficients of each harmonic on the right side have been gathered, the differential equation will have the form (33). The application of the formula (39) yields the constants of the solution (40) in terms of the A_{hj}^2, B_{hj}^2, L_{hj}^1, M_{hj}^1, . . . , L_{hj}^2, M_{hj}^2, . . . of the differential equation. The L_{hj}^3, M_{hj}^3, . . . are then known and are sufficient to determine the L_{hj}, M_{hj}, . . . if the foregoing process is repeated.

MAXIMUM VELOCITY INCREMENT AND CONVERGENCE

For flow over a profile symmetric about the y-axis, the maximum velocity increment occurs at the midchord. At the critical free-stream

Mach number, the flow will be sonic at the midchord, and for higher free-stream Mach numbers, a local supersonic region will develop.

Connected with the formation of this region is the question of convergence of the series obtained from the iteration process to represent the maximum velocity increment. This question of convergence is especially important because the maximum velocity increment is expected to be the first velocity component at any point in the flow to diverge, and this divergence signals the failure of the iteration process to serve as a method of solution. If several terms of a series are known and subsequent terms are assumed to decrease in the same manner, an estimate of the domain of convergence may be made as follows:

The limiting $(\tau \to 0,\ x \to 0)$ perturbation velocity at the midchord is a sum of terms (equations (3), (15), and (30))

$$\lim_{\substack{x \to 0 \\ y \to 0}} \varphi_x^n = -\left[\frac{1}{\sin t}\frac{\partial}{\partial t}\left(\frac{\beta^2}{\Gamma_M}F^n\right)\right]_{\substack{s=0 \\ t=\pi/2}}$$

$$= \frac{\tau}{\beta}K^{n-1}\sum_h\sum_j L_{hj}^n\, h(-1)^{\frac{h-1}{2}}$$

$$\equiv \frac{\tau}{\beta}K^{n-1}\rho^n \tag{41}$$

or

$$\lim_{\substack{x \to 0 \\ y \to 0}} \varphi_x = \frac{\tau}{\beta}\sum_n K^{n-1}\rho^n \tag{42}$$

The ρ^n are seen by definition to depend only on the L_{hj}^n which introduce the effect of the shape of the body. The series (42) will converge if the limit of the ratio of successive terms is less than 1 for all n:

$$\lim_{n \to \infty} \frac{K^n \rho^{n+1}}{K^{n-1}\rho^n} < 1$$

or

$$K_l = \text{g.l.b.} \frac{\rho_n^{n-1}}{\rho} \qquad n \to \infty \tag{43}$$

where K_l is the maximum value of the similarity parameter for which convergence of the iteration process will occur.

The so-called potential limit Mach number, or free-stream Mach number for which the solution diverges for any τ, is defined by

$$\frac{\Gamma_{M_l \tau}}{\beta^3} = K_l$$

or

$$\frac{M_l^2 \left(1 + \frac{\gamma-1}{2} M_l^2\right)}{\left(1 - M_l^2\right)^{3/2}} = \frac{K_l}{\tau} \tag{44}$$

SURFACE VELOCITIES

For small disturbances such that the squares of the perturbation velocities may be neglected compared with unity, the transformed limiting perturbation velocity on the ellipse is

$$F_x(x,0) = -\frac{1}{\sin t} F_t(0,t)$$

$$= \frac{1}{\sin t} \sum_n K^n \sum_h \sum_j^n L_{hj} \, h \sin ht$$

or, in the x,y-plane,

$$\varphi_x(x,0) = \frac{1}{\sin t} \frac{\tau}{\beta} \sum_n K^{n-1} \sum_h \sum_j^n L_{hj} \, h \sin ht \tag{45}$$

Equation (45) will hold only on that portion of the surface along which $J \doteq 1$ (figs. 5 and 6).

The local Mach number at the midchord is given for the small perturbation case by equation (27) of reference 11:

$$M^2 - 1 = - \beta^2 + 2\Gamma_M \varphi_x (0,0) \tag{46}$$

In a previous discussion concerning figure 2 it was seen that the hyperbolic region of the limiting equation (7) represents very nearly the region of supersonic flows for a perfect fluid. Therefore the parabolic curve

$$F_x = \frac{1}{2} \quad \text{or} \quad \varphi_x = \frac{\beta^2}{2\Gamma_M} \tag{47}$$

can be used to outline the supersonic region or to find significant points on it in the physical plane. Whether or not an iteration solution can correctly describe a supersonic flow may be questioned, for as performed here the iteration procedure is essentially the solution of a set of elliptic equations. The applications which follow, although not answering this question directly, do suggest convergence of the solution in the hyperbolic region.

For any thickness ratio τ the critical Mach number, or lowest free-stream Mach number at which some point in the flow field becomes sonic, is given by

$$\frac{\Gamma_M \tau}{\beta^3} = K_c$$

or

$$\frac{M_c^2 \left(1 + \frac{\gamma-1}{2} M_c^2\right)}{(1 - M_c)^{3/2}} = \frac{K_c}{\tau} \tag{48}$$

APPLICATION TO ELLIPTIC CYLINDER

The expression that describes the upper surface of an ellipse whose major axis coincides with the direction of flow is

$$\begin{aligned} y = \tau\, g(x) &= \tau\sqrt{1 - x^2} \\ &= \tau \sin t \qquad (s \to 0) \end{aligned} \tag{49}$$

It follows from equation (27) that

$$F = Ke^{-s}\cos t \qquad (50)$$

Subsequent approximations through the sixth have been calculated by means of the iteration process previously described. The coefficients A_{hj}^{n}, B_{hj}^{n}, and C_{hj}^{n} and the L_{hj}^{n}, M_{hj}^{n}, N_{hj}^{n}, and O_{hj}^{n} calculated by means of equations (33) and (39) are presented in table I in matrix arrangement. From equation (41),

$$\varphi_x(0,0) = \frac{\tau}{\beta}(1 + 0.35237\,K + 0.36986\,K^2 + 0.51836\,K^3 + 0.83711\,K^4 + 1.42014\,K^5 + \ldots) \qquad (51)$$

For comparison, the maximum disturbance velocity as determined by the first three approximations of the iteration solution herein described is plotted (fig. 7) with the exact solution of Hantzsche (reference 12). Hantzsche's iteration process is based on an expansion of the stream function in powers of the thickness ratio. The agreement between the two methods appears close enough to justify the calculation of higher approximations for obtaining a better estimate of the potential limit Mach number.

An estimate is made in figure 8 of the largest value K_ζ of the similarity parameter for which the series for the maximum velocity increment will converge. The broken line joins successive estimates of K_ζ obtained by comparing terms by means of a ratio test described in the section "MAXIMUM VELOCITY INCREMENT AND CONVERGENCE." An examination of the slopes of the segments of the line indicates that the limiting ratio of these slopes, for large n, is about 1/2. If it is assumed that these slopes continue to decrease in a ratio 1/2, the greatest lower bound of the broken line curve can be calculated by a geometric progression. The estimated greatest lower bound of the broken line is then about $K_\zeta = 0.56$.

That the solution converges even when some of the flow is supersonic (hyperbolic) is indicated in figure 9, which shows the contribution of each approximation to the maximum velocity increment for varying K. Supersonic flows lie to the right of the parabolic curve and the intersection of this curve and the sixth approximation marks the value of the parameter K at which the transition from totally subsonic flows to partly supersonic flows occurs. This transition

point, $K_c \doteq 0.395$, is also very evident in figure 10 as the intersection of the curves, for several values of M_0, of the local Mach number at midchord (equations (42) and (46)).

The surface velocity on the ellipse for three values of K is presented in figure 11. The parabolic line, equation (47), is included in each case for comparison. Thus in figure 11(a) all velocities are subsonic, whereas figure 11(b) (K = 0.4) shows a partly supersonic flow. This is in agreement with the previous calculation showing transition from subsonic flow to supersonic flow at $K_c = 0.395$. The longitudinal extent of the symmetric supersonic region is seen to be about 1/10 chord, based on six approximations. The last of this series of figures (fig. 11(c)) is for a value of K near K_1. Although the series for the velocity increment may be converging, it is evident that near the midchord the uncalculated approximations are not negligible for this value of K. The width of the supersonic region is greater than the extent of the region of accuracy of the calculations.

Curves of critical Mach number and potential limit Mach number against thickness ratio have been plotted in figure 12 using equations (48) and (44), respectively.

APPLICATION TO KAPLAN BUMP

As a second example, the iteration process is applied to the calculation of noncirculatory flow past a Kaplan section; this problem has been treated in an exact manner to three approximations in reference 4. The Kaplan section has no stagnation points (fig. 5) so that nowhere is the boundary condition singular. Its parametric representation is (reference 4),

$$\left.\begin{aligned} x &= \cos t \\ y &= \frac{\tau}{4}(3 \sin t - \sin 3t) \end{aligned}\right\} \qquad (52)$$

Application of equation (27) yields

$$\frac{1}{F} = \frac{K}{4}(3e^{-s} \cos t - e^{-3s} \cos 3t) \qquad (53)$$

The second, third, and fourth approximations have been calculated according to the procedure given in the section "HIGHER APPROXIMATIONS" and are recorded in table II as arrays of the constants L_{hj}^{n}, M_{hj}^{n}, and N_{hj}^{n}. The constants A_{hj}^{n}, B_{hj}^{n}, and C_{hj}^{n} represent the nonhomogeneous terms of the differential equations (33).

The chordwise perturbation-velocity distribution at the surface is plotted in figure 13 for comparison with the result of Kaplan (reference 4) for $\tau = 0.10$ and $M_0 = 0.75$. The agreement is probably sufficient from a practical standpoint to justify the labor-saving limiting processes that have been made in the iteration process.

An estimate of the limiting value of the parameter K for which the series for the maximum velocity increment will converge is made in figure 14, where the ratios of successive coefficients in the series for the maximum velocity increment are plotted for the first four terms. The series for $(\varphi_x)_{max}$ to four approximations is calculated from equation (41) to be

$$(\varphi_x)_{max} = \frac{\tau}{\beta}\left(\frac{3}{2} + 0.81762\ K + 1.15715\ K^2 + 2.11564\ K^3 + \ldots\right) \quad (54)$$

An analysis similar to that employed on the corresponding series for the elliptic cylinder indicates that the series (56) will converge for values of $K < 0.387$.

The value $K_l = 0.387$ is considerably above the value of K for which the flow becomes sonic at the midchord, as given in figure 15 by the intersection of the fourth approximation curve and the parabolic curve. The converging nature of the successive approximations indicates that this value of $K_c = 0.270$ will be lowered only slightly by increased accuracy from higher-order terms.

The variation of the local Mach number corresponding to the maximum velocity increment has been calculated by means of equation (46) and is plotted against the similarity parameter for several values of free-stream Mach number in figure 16. The calculations are based on four approximations. The velocity increment on the surface of the bump is plotted as a function of distance along the chord in figure 17. Of these, figure 17(a) shows the only completely subsonic flow. In figure 17(b), $K_c < K = 0.3 < K_l$. Hence the flow is everywhere convergent, but near the midchord there is a small supersonic region represented by those values of $(F_x)_{max}$ above the parabolic curve. For figure 17(c), the similarity parameter is chosen slightly larger than the estimated maximum for convergence, K_l, as obtained from equation (43) and figure 14; and, although successive approximations still decrease monotonically, the curves of figure 17(c) should not be expected ultimately to converge.

Figure 18 shows the critical Mach number M_c and the potential limit Mach number M_l as functions of thickness ratio. For comparison, M_c and M_l as computed by Kaplan (reference 4) are included. The present calculations indicate that isentropic mixed flow is restricted to a considerably smaller range of Mach number.

CONCLUDING REMARKS

An iteration procedure similar to that employed in the Ackeret-Prandtl type procedure has been utilized in the calculation of the symmetric-type transonic potential flow for an elliptic cylinder and a Kaplan section. In order to obtain an estimate of the region of convergence of this type of solution, the work has been carried through six approximations for the elliptic cylinder and through four approximations for the Kaplan section.

The results indicate that the iteration solution converges for a range of the similarity parameter for which supersonic regions exist in the flow field. For these hyperbolic regions, the nonlinear term of the potential equation is not, strictly speaking, small compared with either term of the Laplacian. The iteration procedure presented herein may therefore be applicable to a greater range of disturbance velocities than would be indicated by its method of formulation, in which the nonlinear term is considered a perturbation on the Laplacian.

The results have been presented in conformity with the transonic similarity law. The essential characteristics of a flow may then be presented in a simple and direct manner by classifying the flow with respect to significant values of the similarity parameter, for example, the critical and potential limit values.

Lewis Flight Propulsion Laboratory
National Advisory Committee for Aeronautics
Cleveland, Ohio, June 26, 1951

APPENDIX - SYMBOLS

The following symbols are used in this report:

A,B,C	constants
c^*	critical velocity
F	perturbation potential in $x\eta$-plane
f	function of x,η
g	thickness distribution along chord
g.l.b.	greatest lower bound
$J\left(\frac{x,\eta}{s,t}\right)$	functional determinant, or Jacobian
K	transonic similarity parameter
K_c	critical value of similarity parameter
K_l	potential limit of similarity parameter
L,M,N,O	constants, identified by superscripts and subscripts
M	local Mach number
M_c	critical Mach number
M_l	potential limit Mach number
M_0	free-stream Mach number
n	number of approximations
P	particular integral
q	function of s
s,t	elliptic coordinates
U	free-stream velocity
x,y	cartesian coordinates
β	$\sqrt{1 - M_0^2}$

Γ_M	$M_0^2(1 + \frac{\gamma-1}{2} M_0^2)$
γ	ratio of specific heats
Δ	Laplacian
δ	constant
η	transformed y-coordinate
τ	thickness ratio
φ	perturbation potential
ω,ρ,σ	constants, identified by subscripts

Subscripts:

x,y,η,s,t	indicate partial derivatives
h,j,k,m,p,r,ν	summation indices

Superscripts:

λ,n,ν	number of approximation

REFERENCES

1. Wang, Chi-Teh: Variational Method in the Theory of Compressible Fluid. Jour. Aero. Sci., vol. 15, no. 11, Nov. 1948, pp. 675-685.

2. Liepmann, Hans Wolfgang, and Puckett, Allen E.: Introduction to Aerodynamics of a Compressible Fluid. John Wiley & Sons, Inc., 1947.

3. Ackeret, J.: Über Luftkräfte bei sehr grossen Geschwindigkeiten insbesondere bei ebenen Strömungen. Helvetica Physica Acta, vol. I, fasc. 5, 1928, P. 301-322.

4. Kaplan, Carl: The Flow of a Compressible Fluid past a Curved Surface. NACA Rep. 768, 1943.

5. Perl, W., and Klein, Milton M.: Theoretical Investigation and Application of Transonic Similarity Law for Two-Dimensional Flow. NACA TN 2191, 1950.

6. von Kármán, Theodore: The Similarity Law of Transonic Flow. Jour. Math. Phys., vol XXVI, no. 3, Oct. 1947, pp. 182-190.

7. Sears, W. R.: Transonic Potential Flow of a Compressible Fluid. Jour. Appl. Phys., vol. 21, no. 8, Aug. 1950, pp. 771-778.

8. Kuo, Yung-Huai: On the Stability of Two-Dimensional Smooth Transonic Flows. Jour. Aero. Sci., vol. 18, no. 1, Jan. 1951, pp. 1-6.

9. Beavan, J. A., and Hyde, G. A. M.: Examples of Pressure Distributions at Compressibility Speeds on EC 1250. R. & M. No. 2056, British A.R.C., 1942.

10. Beavan, J. A., Hyde, G. A. M., and Fowler, R. G.: Pressure and Wake Measurements up to Mach Number 0.85 on an EC 1250 Section with 25 per cent Control. R. & M. No. 2065, British A.R.C., 1945.

11. Perl, William: Calculation of Transonic Flows Past Thin Airfoils by an Integral Method. NACA TN 2130, 1950.

12. Hantzsche, W.: Die Prandtl-Glauertsche Näherung als Grundlage für ein Iterationsverfahren zur Berechnung kompressibler Unterschallströmungen. Z.f.a.M.M., Bd. 23, Nr. 4, Aug. 1943, S. 185-199.

TABLE I - FIRST APPROXIMATION FOR ELLIPSE

(a) $A^{1}_{1j} = B^{1}_{1j} = 0$ (b) $L^{1}_{11} = 1.0$

TABLE II - SECOND APPROXIMATION FOR ELLIPSE

(a) A^{2}_{hj}

h \ j	2
1	-0.50000
3	0.75000
5	-0.25000

(b) L^{2}_{hj}

h \ j	1	2	3	4	5
1	0.33333	-0.16667	---	---	---
3	---	-0.15000	0.10000	---	---
5	---	0.01190	---	---	-0.00476

TABLE III - THIRD APPROXIMATION FOR ELLIPSE

(a) A^{3}_{hj}

h \ j	2	3	4	5	6
1	-0.33333	-0.18571	0.22500	---	0.00595
3	0.50000	0.86667	-0.67500	---	-0.04167
5	-0.16667	-0.15238	0.67500	---	0.08929
7	---	0.53095	-0.22500	---	-0.19118
9	---	-0.05952	---	---	0.02381

(b) L^{3}_{hj}

h \ j	1	2	3	4	5	6	7	9
1	0.23084	-0.11111	-0.02321	0.1500	---	0.00017	---	---
3	---	-0.10000	0.15018	-0.09643	---	-0.00154	---	---
5	---	0.00794	0.07202	-0.07500	0.00388	0.00812	---	---
7	---	---	-0.01327	0.00682	---	0.00595	-0.00331	---
9	---	---	0.00083	---	---	-0.00053	---	0.00007

TABLE IV - FOURTH APPROXIMATION FOR ELLIPSE

(a) A^{4}_{hj}

h \ j	2	3	4	5	6	7	8	9	10
1	0.14520	0.09288	-0.16301	0.04985	0.01268	0.00436	0.00179	---	0.00007
3	-0.21480	-0.43335	0.31663	0.02354	-0.02353	-0.02820	-0.00936	---	-0.00007
5	0.07160	0.57662	0.19904	-0.52948	0.06649	0.02305	0.03632	---	0.00024
7	---	-0.26551	-0.75659	0.80078	-0.07488	0.05956	-0.07065	---	-0.00132
9	---	0.02977	0.49494	-0.38547	0.02823	-0.10221	0.06084	---	0.00262
11	---	---	-0.09795	0.04100	---	0.04808	-0.01895	---	-0.00222
13	---	---	0.00693	---	---	-0.00464	---	---	0.00069

(b) B^{4}_{hj}

h \ j	4
1	0.16250
3	-0.48749
5	0.48749
7	-0.16250

(c) L^{4}_{hj}

h \ j	1	2	3	4	5	6	7	8	9	10	11	12	13
1	0.22498	-0.09547	-0.02332	0.01018	-0.00414	-0.00072	-0.00018	-0.00006	---	-0.00000	---	---	---
3	---	-0.08592	-0.04018	0.06871	-0.00294	0.00241	0.00141	0.00034	---	0.00000	---	---	---
5	---	0.00682	0.07203	-0.05206	0.01638	-0.01209	-0.00192	-0.00186	---	-0.00001	---	---	---
7	---	---	-0.01328	-0.04347	0.00673	-0.01152	-0.01829	0.00942	---	0.00005	---	---	---
9	---	---	0.00083	0.01523	-0.01377	0.00125	-0.00639	0.00716	-0.00132	-0.00028	---	---	---
11	---	---	---	-0.00187	0.00085	---	0.00134	-0.00086	---	-0.00021	0.00012	---	---
13	---	---	---	0.00009	---	---	-0.00008	---	---	0.00002	---	---	-0.00000

(d) M^{4}_{hj}

h \ j	3	4	5	6	7
1	---	-0.02167	---	---	---
3	-0.14445	0.13928	---	---	---
5	---	0.10833	-0.10590	---	---
7	---	-0.00985	---	---	0.00851

TABLE V - FIFTH APPROXIMATION FOR ELLIPSE

(a) A^{5}_{hj}

h \ j	2	3	4	5	6	7	8	9	10	11	12	13	14
1	-0.30193	-0.19052	-0.04166	0.16208	0.01156	0.00285	0.00531	0.00204	0.00196	0.00004	0.00028	---	---
3	0.45289	0.88909	0.58486	-0.74174	-0.11238	-0.02831	0.02488	-0.03838	-0.00891	0.00041	-0.00066	---	---
5	-0.15098	-1.18221	-1.98028	1.18749	0.75422	0.01647	-0.27282	0.16484	0.02092	0.00200	0.00086	---	---
7	---	0.54470	2.49445	0.21268	-2.59319	0.34671	0.49167	-0.15302	-0.05639	-0.01005	-0.00175	---	---
9	---	-0.08107	-1.32017	-2.07283	3.52376	-0.63624	-0.11714	-0.21780	0.10470	0.00985	0.00719	---	0.00003
11	---	---	0.26125	1.67599	-1.93465	0.33485	-0.34649	0.43170	-0.09089	0.00799	-0.01371	---	-0.00015
13	---	---	-0.01847	-0.48297	0.57619	-0.03630	0.25889	-0.20890	0.02862	-0.01837	0.01153	---	0.00025
15	---	---	---	0.06256	-0.02532	---	-0.04744	0.01972	---	0.00892	-0.00354	---	-0.00019
17	---	---	---	-0.00327	---	---	0.00290	---	---	-0.00079	---	---	0.00005

(b) B^{5}_{hj}

h \ j	4	5	6	7	8
1	0.43334	0.14341	0.19737	---	0.00516
3	1.30002	0.08802	-1.05859	---	-0.04010
5	-1.30002	-1.52956	2.24554	---	0.17670
7	0.43334	2.31317	-2.04580	---	-0.34109
9	---	-1.11344	0.85948	---	0.28868
11	---	0.11840	---	---	-0.08735

TABLE V - FIFTH APPROXIMATION FOR ELLIPSE - Concluded

(c) L^5_{hj}

h \ j	1	2	3	4	5	6	7	8	9	10	11	12	13	14	15	17
1	0.26680	-0.10064	-0.02581	-0.01818	0.00824	0.00226	0.00006	0.00010	0.00003	0.00002	0.00000	0.00000	---	---	---	---
3	---	-0.09058	0.21449	0.29580	-0.04370	-0.02153	-0.00071	0.00024	-0.00063	-0.00010	0.00000	-0.00000	---	---	---	---
5	---	0.00719	0.07589	0.08941	-0.41898	0.29128	0.00069	-0.00613	0.00294	0.00028	0.00002	0.00000	---	---	---	---
7	---	---	-0.01382	-0.07241	0.05120	0.05421	-0.02332	0.00882	-0.00478	-0.00111	-0.00014	-0.00002	---	---	---	---
9	---	---	0.00085	0.02051	0.03348	-0.07440	0.01998	0.02276	-0.02052	0.00551	0.00025	0.00011	---	0.00000	---	---
11	---	---	---	-0.00249	-0.01733	0.02278	-0.00485	0.00565	-0.01079	0.00433	0.00078	-0.00060	---	-0.00000	---	---
13	---	---	---	0.00012	0.00335	-0.00285	0.00030	-0.00248	0.00237	-0.00042	0.00058	-0.00046	0.00010	0.00001	---	---
15	---	---	---	---	-0.00031	0.00015	---	0.00030	-0.00014	---	-0.00009	0.00004	---	0.00001	-0.00000	---
17	---	---	---	---	0.00001	---	---	-0.00001	---	---	0.00000	---	---	-0.00000	---	-0.00000

(d) M^5_{hj}

h \ j	3	4	5	6	7	8	9	10	11
1	---	-0.02889	0.00698	0.00584	---	0.00008	---	---	---
3	-0.14818	0.18578	0.00426	-0.03913	---	-0.00073	---	---	---
5	---	0.14446	-0.10545	0.20414	---	0.00453	---	---	---
7	---	-0.01513	-0.09838	0.18737	-0.02476	-0.02274	---	---	---
9	---	---	0.01988	---	---	-0.01686	0.01210	---	---
11	---	---	-0.00123	---	---	0.00154	---	---	-0.00038

(e) N^5_{hj}

$N^5_{55} = 0.07848$

$N^5_{hj} = 0;\ h,j \neq 5$

TABLE VI - SIXTH APPROXIMATION FOR ELLIPSE

(a) A^{6}_{hj}

h \ j	2	3	4	5	6	7	8	9
1	-0.35512	-0.20367	-0.54907	0.53760	0.52224	0.39212	0.01983	-0.00962
3	0.53268	0.95047	2.16610	-1.13329	-3.53878	2.24494	0.27821	-0.05669
5	-0.17756	-1.26381	-3.67930	-0.80210	8.32920	-3.82950	-0.96660	0.19693
7	---	0.58229	3.23792	4.50042	-8.29361	0.43150	1.86413	0.21831
9	---	-0.06528	-1.43991	-5.29265	1.98519	6.03432	-2.58489	-0.95363
11	---	---	0.28437	2.85636	2.82542	-7.73804	2.34101	0.50963
13	---	---	-0.02010	-0.75951	-2.64252	4.22655	-1.11805	0.50443
15	---	---	---	0.09828	0.97957	-1.11033	0.22088	-0.54201
17	---	---	---	-0.00511	-0.18374	0.13964	-0.01486	0.14955
19	---	---	---	---	0.01776	-0.00697	---	-0.01773
21	---	---	---	---	-0.00072	---	---	0.00082

(a) A^{6}_{hj} - Concluded

h \ j	10	11	12	13	14	15	16	18
1	0.00467	-0.00511	0.00088	-0.00052	-0.00014	-0.00002	-0.00000	-0.00000
3	0.00801	0.01975	0.00047	0.00045	0.00043	0.00006	0.00002	0.00000
5	-0.02668	-0.05440	-0.01173	0.00009	-0.00080	-0.00001	-0.00007	-0.00000
7	-0.33773	0.17216	0.01806	0.00866	0.00131	-0.00007	0.00008	0.00000
9	0.69461	-0.17444	0.00844	-0.03344	-0.00290	-0.00018	-0.00005	-0.00000
11	0.11262	-0.17842	-0.02885	0.03281	0.00916	0.00084	0.00007	0.00000
13	-1.00872	0.39807	-0.01228	0.02266	-0.01671	-0.00085	-0.00029	0.00001
15	0.66684	-0.19573	0.05158	-0.05514	0.01389	-0.00039	0.00059	-0.00003
17	-0.12088	0.01812	-0.03191	0.02680	-0.00423	0.00115	-0.00053	0.00004
19	0.00725	---	0.00568	-0.00239	---	-0.00057	0.00017	-0.00003
21	---	---	-0.00033	---	---	0.00005	---	0.00001

TABLE VI - SIXTH APPROXIMATION FOR ELLIPSE - Continued

(b) B^{6}_{hj}

h \ j	4	5	6	7	8	9	10	12
1	-0.44175	0.27651	0.17244	-0.21716	-0.07427	0.00325	-0.01077	-0.00071
3	1.32524	0.07448	-0.95724	1.36008	0.22528	0.09495	0.02864	0.00142
5	-1.32524	-2.37617	1.17188	-1.02543	-0.60779	-0.40598	-0.11295	-0.00071
7	0.44175	3.51929	1.55575	-3.43737	1.21433	0.34626	0.45626	0.00399
9	---	-1.66999	-3.93061	5.82295	-1.13510	0.47585	-0.84175	-0.02074
11	---	0.17588	2.42446	-2.77921	0.37754	-0.89299	0.69364	0.02897
13	---	---	-0.46759	0.27615	---	0.41725	-0.20907	-0.03169
15	---	---	0.03092	---	---	-0.03859	---	0.00947

(c) C^{6}_{hj}

h \ j	
1	-0.38239
3	1.24277
5	-1.43397
7	0.66918
9	-0.09560

TABLE VI - SIXTH APPROXIMATION FOR ELLIPSE - Continued

(d) L^{6}_{hj}

h \ j	1	2	3	4	5	6	7	8	9	10
1	0.34464	-0.11837	-0.02546	-0.05231	0.02720	0.01467	-0.00949	-0.00061	-0.00011	0.00003
3	---	-0.10654	-0.40107	0.52581	-0.06792	-0.13205	0.06802	0.00625	-0.00046	0.00016
5	---	0.00846	0.07899	0.27792	-0.66704	0.58684	-0.18449	-0.03118	0.00119	-0.00076
7	---	---	-0.01456	-0.09487	-0.12642	0.65280	-0.67976	0.21063	0.01291	-0.00314
9	---	---	0.00091	0.02215	0.08919	-0.06701	-0.10896	0.08921	0.00838	-0.01008
11	---	---	---	-0.00271	-0.02956	-0.02921	0.09997	-0.03921	-0.02279	0.02609
13	---	---	---	0.00013	0.00527	0.01955	-0.03495	0.01065	-0.00476	0.01374
15	---	---	---	---	-0.00049	-0.00517	0.00631	-0.00137	0.00373	-0.00533
17	---	---	---	---	0.00002	0.00073	-0.00058	0.00007	-0.00064	0.00063
19	---	---	---	---	---	-0.00005	0.00002	---	0.00006	-0.00005
21	---	---	---	---	---	0.00000	---	---	-0.00000	---

(d) L^{6}_{hj} - Concluded

h \ j	11	12	13	14	15	16	17	18	19	21
1	-0.00004	0.00001	-0.00000	-0.00000	-0.00000	-0.00000	---	-0.00000	---	---
3	0.00018	0.00000	0.00000	0.00000	0.00000	0.00000	---	0.00000	---	---
5	-0.00057	-0.00010	0.00000	-0.00000	-0.00000	-0.00000	---	-0.00000	---	---
7	0.00239	0.00020	0.00007	0.00001	-0.00000	0.00000	---	0.00000	---	---
9	-0.00436	0.00001	-0.00038	-0.00003	-0.00000	-0.00000	---	-0.00000	---	---
11	-0.01128	0.00051	0.00068	0.00012	0.00001	0.00000	---	0.00000	---	---
13	-0.00829	-0.00073	0.00227	-0.00062	-0.00002	-0.00000	---	0.00000	---	---
15	0.00188	-0.00060	0.00098	-0.00048	0.00001	0.00002	---	-0.00000	---	---
17	-0.00011	0.00022	-0.00022	0.00005	-0.00002	0.00002	-0.00000	0.00000	---	---
19	---	-0.00003	0.00001	---	0.00000	-0.00000	---	0.00000	0.00001	---
21	---	0.00000	---	---	-0.00000	---	---	-0.00000	---	0.00000

TABLE VI - SIXTH APPROXIMATION FOR ELLIPSE - Concluded

(e) M^{6}_{hj}

h \ j	3	4	5	6	7	8	9	10	11	12	13	15
1	---	-0.02945	0.01152	-0.00256	-0.00452	-0.00118	0.00004	-0.00011	---	-0.00000	---	---
3	-0.15841	0.18932	0.00465	0.00546	0.03400	0.00410	0.00132	0.00031	---	0.00001	---	---
5	---	0.14725	0.10397	-0.17789	-0.04273	-0.01558	-0.00725	-0.00151	---	-0.00001	---	---
7	---	-0.01339	-0.14864	-0.11867	-0.02132	0.04857	0.01082	0.00887	---	0.00004	---	---
9	---	---	0.02982	0.08621	-0.18197	0.08677	0.05151	-0.04430	---	-0.00033	---	---
11	---	---	-0.00183	-0.02852	0.03860	-0.00662	0.02232	-0.03303	0.00811	0.00169	---	---
13	---	---	---	0.00352	-0.00230	---	-0.00474	0.00303	---	0.00127	-0.00087	---
15	---	---	---	-0.00018	---	---	0.00027	---	---	-0.00012	---	0.00001

(f) N^{6}_{hj}

h \ j	5	6	7	9
1	---	-0.01093	---	---
3	---	0.04603	---	---
5	0.11881	-0.13036	---	---
7	---	-0.05148	0.12276	---
9	---	0.00212	---	-0.01322

TABLE VII - FIRST APPROXIMATION FOR KAPLAN SECTION

(a) $A^{1}_{hj} = 0$

(b) L^{1}_{hj}

h \ j	1	3
1	0.75000	---
3	---	-0.25000

TABLE VIII - SECOND APPROXIMATION FOR KAPLAN SECTION

(a) $A^{2}_{hj}\left(\frac{8}{3}\right)^{2}$

h \ j	2	4	6
1	-2	-3	-1
3	3	9	2
5	-1	-9	-4
7	0	3	5
9	0	0	-2

(b) L^{2}_{hj}

e^{-s}	1	2	3	4	5	6	7	9
1	0.32412	-0.09375	---	-0.02813	---	-0.00402	---	---
3	---	-0.08438	-0.20566	0.18081	---	0.01042	---	---
5	---	0.00670	---	0.14063	-0.05382	-0.05114	---	---
7	---	---	---	-0.01278	---	-0.05409	0.05367	---
9	---	---	---	---	---	0.00625	---	-0.00417

TABLE IX - THIRD APPROXIMATION FOR KAPLAN SECTION

(a) $^{3}A_{hj}$

h \ j	2	3	4	5	6	7	8	9	10	11	12
1	-0.24306	-0.07635	-0.34704	-0.07433	-0.18091	-0.28897	-0.20181	0.06150	-0.14087	---	---
3	0.38462	0.36563	1.22344	0.14304	-0.00618	0.48560	-0.49403	0.24413	-0.56348	---	-0.02108
5	-0.12154	-0.46618	-1.34498	-1.41705	0.17837	-0.33128	1.02705	-0.55314	0.27545	---	0.07734
7	---	0.22400	0.46858	2.10642	0.15390	1.43784	-1.86276	0.20798	-0.58862	---	-0.08141
9	---	-0.02611	---	-1.01775	-0.14524	-2.49763	1.70192	-0.37881	0.98463	---	0.06328
11	---	---	---	0.10901	---	1.32190	-0.55398	0.87875	-1.08332	---	-0.09844
13	---	---	---	---	---	-0.14718	---	-0.52568	-0.13089	---	0.11250
15	---	---	---	---	---	---	---	0.06328	---	---	-0.04219

(b) $^{3}L_{hj}$

h \ j	1	2	3	4	5	6	7	8	9	10	11	12	13	14
1	0.89487	-0.08103	-0.00878	-0.02314	0.00310	-0.00617	-0.00602	0.00320	0.00077	0.00142	---	---	---	---
3	---	-0.07282	-0.21244	0.17478	0.00884	-0.00023	0.01213	-0.00698	0.00339	0.00619	---	-0.00016	---	---
5	---	0.00679	0.05039	0.14944	-0.15715	0.01822	-0.01380	0.02635	-0.00988	0.00987	---	0.00085	---	---
7	---	---	-0.00560	-0.01420	-0.00785	-0.01184	0.22204	-0.12552	0.00650	-0.01174	---	-0.00098	---	---
9	---	---	0.00035	---	0.01817	0.00323	0.07806	-0.10011	-0.03949	0.05077	---	0.00100	---	---
11	---	---	---	---	-0.00114	---	-0.01836	0.00972	-0.02187	0.06063	-0.01826	-0.00428	---	---
13	---	---	---	---	---	---	0.00123	---	0.00595	0.00189	---	-0.00460	-0.00206	---
15	---	---	---	---	---	---	---	---	-0.00044	---	---	0.00052	---	-0.00015

(c) $^{3}M_{hj}$

h \ j	3	5	7	9
3	-0.08094	---	---	---
5	---	0.14170	---	---
7	---	---	-0.10413	---
9	---	---	---	0.02105

TABLE I - FOURTH APPROXIMATION FOR KAPLAN SECTION

(a) A^4_{hj}

h \ j	2	3	4	5	6	7	8	9
1	-0.27369	-0.10158	-0.70184	0.16384	-0.25999	-0.08941	0.27562	0.00827
3	0.41053	0.47402	2.21465	0.20698	-0.14470	0.34639	-0.94946	0.74600
5	-0.13684	-0.63029	-2.54101	-2.37393	-0.09017	-0.37686	3.50541	-2.30284
7	---	0.29040	1.28382	3.50709	2.64389	-6.52365	1.77718	-2.32167
9	---	-0.03256	-0.31320	-1.68637	-3.74815	-3.76360	2.16703	1.62381
11	---	---	0.06195	0.18240	1.95475	2.08185	4.82315	-3.15023
13	---	---	-0.00437	---	-0.38139	-0.24116	-4.05218	1.40343
15	---	---	---	---	0.02576	---	0.80760	-0.10562
17	---	---	---	---	---	---	-0.05443	---
19	---	---	---	---	---	---	---	---
21	---	---	---	---	---	---	---	---

(a) A^4_{hj} - Concluded

h \ j	10	11	12	13	14	15	16	18
1	0.30919	-0.13252	-0.03337	-0.00519	-0.03780	0.00311	-0.00705	-0.00035
3	-1.56053	0.63407	-0.17619	0.30166	0.04789	0.00980	0.01409	0.00035
5	1.92675	-0.67733	0.58936	-0.64026	-0.13063	-0.06476	-0.00705	---
7	1.37105	1.37105	-0.18288	0.12860	0.42178	0.09728	-0.02032	---
9	5.14985	-2.08886	-0.71016	-0.22855	-0.46413	0.00347	0.07111	-0.00280
11	-2.88950	-2.33567	0.76885	1.04169	0.41837	-0.03373	-0.07825	0.00796
13	-3.37322	6.15880	-0.99893	0.85868	-0.95828	-0.07389	0.02888	-0.00818
15	3.42262	-5.15298	1.55071	-2.77829	1.12471	-0.09933	-0.01642	0.00786
17	-0.71285	0.22345	-1.01520	1.34638	-0.42191	0.32418	0.02302	-0.01576
19	0.04935	---	0.22411	-0.02672	---	-0.18607	-0.00802	0.01698
21	---	---	-0.01630	---	---	0.01994	---	-0.00606

(b) B^4_{hj}

h \ j	4	6	8	10	12
1	0.01714	0.02471	0.02657	0.00976	---
3	-0.05142	-0.11585	-0.07267	-0.01881	-0.00395
5	0.05142	0.24498	0.17382	0.07426	0.01578
7	-0.01714	-0.22984	-0.35115	-0.09793	-0.01973
9	---	0.07599	0.33867	0.18995	0.01776
11	---	---	-0.11524	-0.19764	-0.03354
13	---	---	---	0.07041	0.03749
15	---	---	---	---	-0.01381

TABLE X - FOURTH APPROXIMATION FOR KAPLAN SECTION - Concluded

(c) L^{4}_{hj}

h \ j	1	2	3	4	5	6	7	8	9	10
1	0.37947	-0.09125	-0.01270	-0.04618	0.00685	-0.00719	-0.00186	0.00450	0.00010	0.00514
3	---	-0.08211	-0.36592	0.30799	0.01294	-0.00727	0.00866	-0.01764	0.01036	-0.01727
5	---	0.00652	0.03939	0.28741	-0.30613	0.01610	-0.01570	0.09171	-0.04112	0.02595
7	---	---	-0.00726	-0.03903	-0.14613	-0.21970	-0.78172	-0.45988	0.05554	-0.04827
9	---	---	0.00045	0.00482	0.03011	0.08574	0.11761	-0.10872	-0.30580	0.27104
11	---	---	---	-0.00059	-0.00190	-0.02300	-0.02891	-0.08519	0.07876	0.12864
13	---	---	---	0.00005	---	0.00287	0.00201	0.03859	-0.01595	0.04919
15	---	---	---	---	---	-0.00014	---	-0.00502	0.00073	-0.02738
17	---	---	---	---	---	---	---	0.00024	---	0.00577
19	---	---	---	---	---	---	---	---	---	-0.00019
21	---	---	---	---	---	---	---	---	---	---

(c) L^{4}_{hj} - Concluded

h \ j	11	12	13	14	15	16	17	18	19	21
1	-0.00110	-0.00023	-0.00002	-0.00019	0.00001	-0.00003	---	-0.00000	---	---
3	0.00568	-0.00130	0.00189	0.00026	0.00005	0.00006	---	0.00000	---	---
5	-0.00706	0.00498	-0.00445	-0.00076	-0.00082	-0.00011	---	---	---	---
7	0.01904	-0.00198	0.00107	0.00287	0.00035	-0.00010	---	---	---	---
9	-0.05222	-0.01127	-0.00260	-0.00404	0.00002	0.00041	---	-0.00001	---	---
11	-0.14319	0.03191	0.02170	0.00558	-0.00032	-0.00058	---	0.00004	---	---
13	-0.12851	0.04140	0.05407	-0.03549	-0.00132	0.00033	---	-0.00005	---	---
15	0.03032	-0.01919	0.04961	-0.03878	0.00756	-0.00053	---	0.00008	---	---
17	-0.00133	0.00700	-0.01122	0.00454	-0.00507	-0.00070	0.00404	-0.00045	---	---
19	---	-0.00105	0.00014	---	0.00157	0.00008	---	-0.00046	-0.00008	---
21	---	0.00008	---	---	-0.00009	---	---	0.00005	---	-0.00002

(d) M^{4}_{hj}

h \ j	3	4	5	6	7	8	9	10	11	12	13	15
1	---	0.00114	---	0.00071	---	0.00042	---	0.00010	---	---	---	---
3	-0.07900	-0.00735	---	-0.00429	---	-0.00132	---	-0.00054	---	-0.00005	---	---
5	---	-0.00571	0.23739	0.02227	---	0.00446	---	0.00099	---	0.00013	---	---
7	---	0.00052	---	0.01768	-0.14591	-0.02341	---	-0.00192	---	-0.00021	---	---
9	---	---	---	-0.00189	---	-0.01992	-0.09021	0.01000	---	0.00028	---	---
11	---	---	---	---	---	0.00202	---	0.00941	0.10617	-0.00146	---	---
13	---	---	---	---	---	---	---	-0.00102	---	-0.00150	-0.03303	---
15	---	---	---	---	---	---	---	---	---	0.00017	---	0.00331

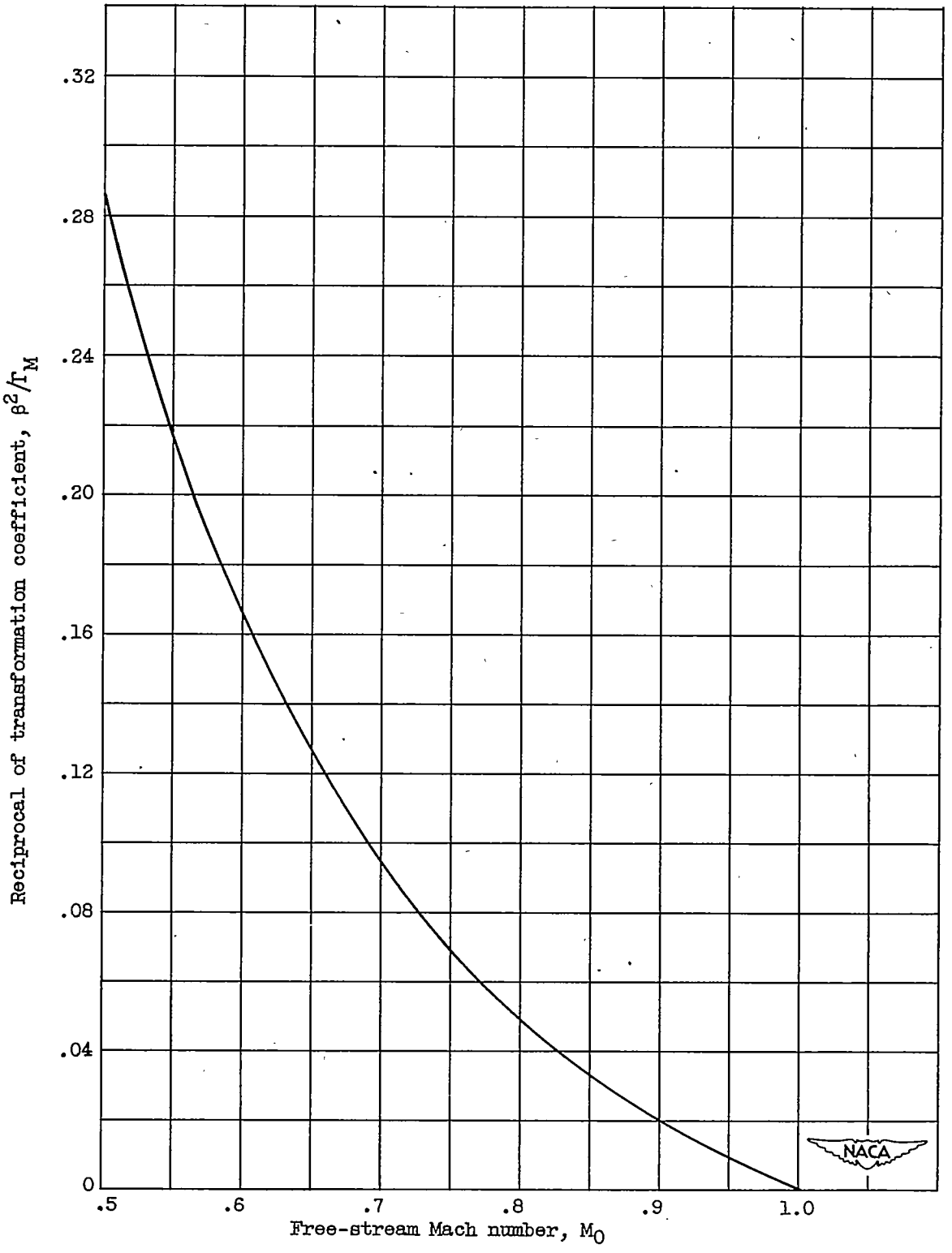

Figure 1. - Reciprocal of transformation coefficient.

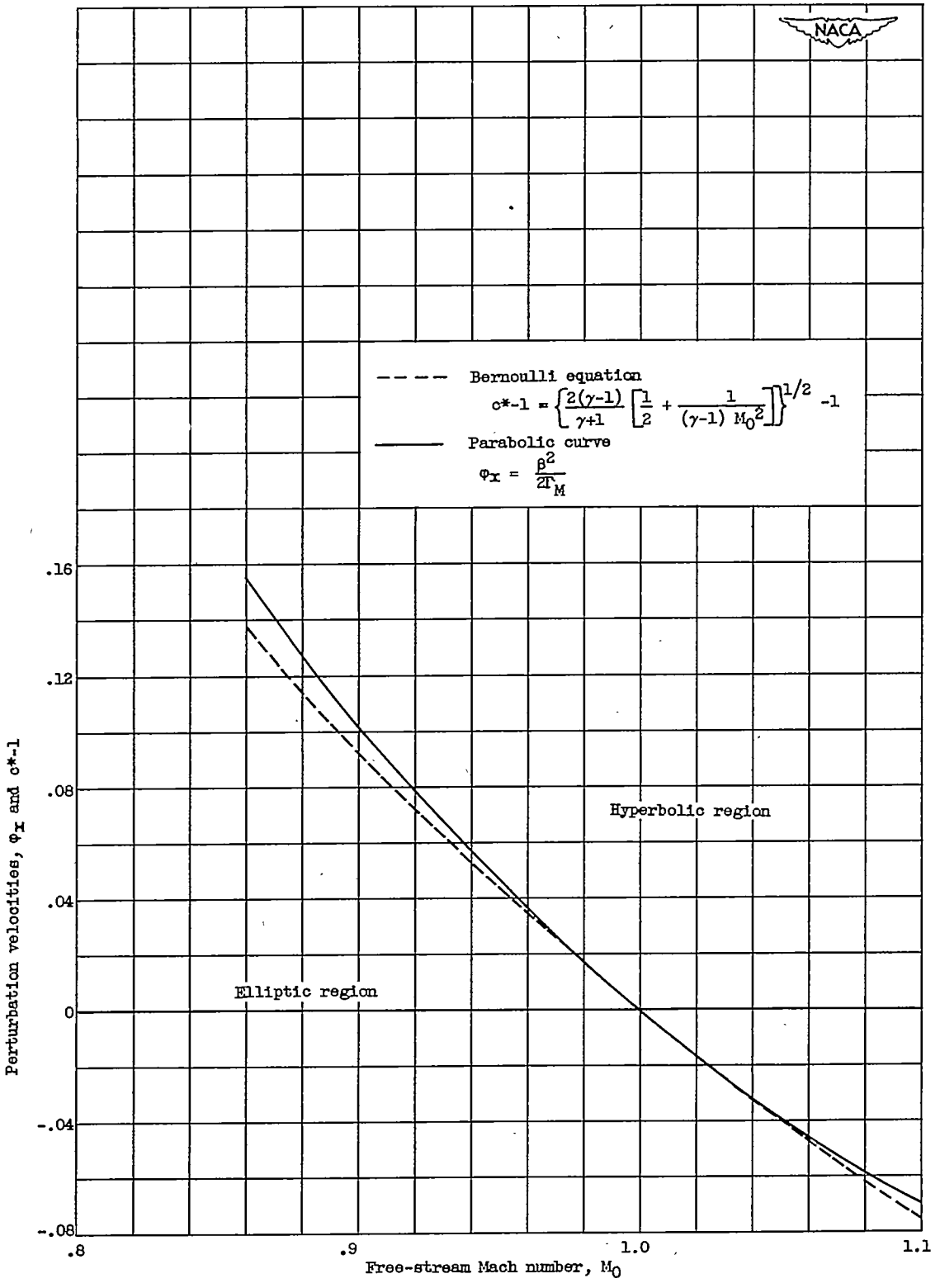

Figure 2. - Parabolic curve of transonic equation.

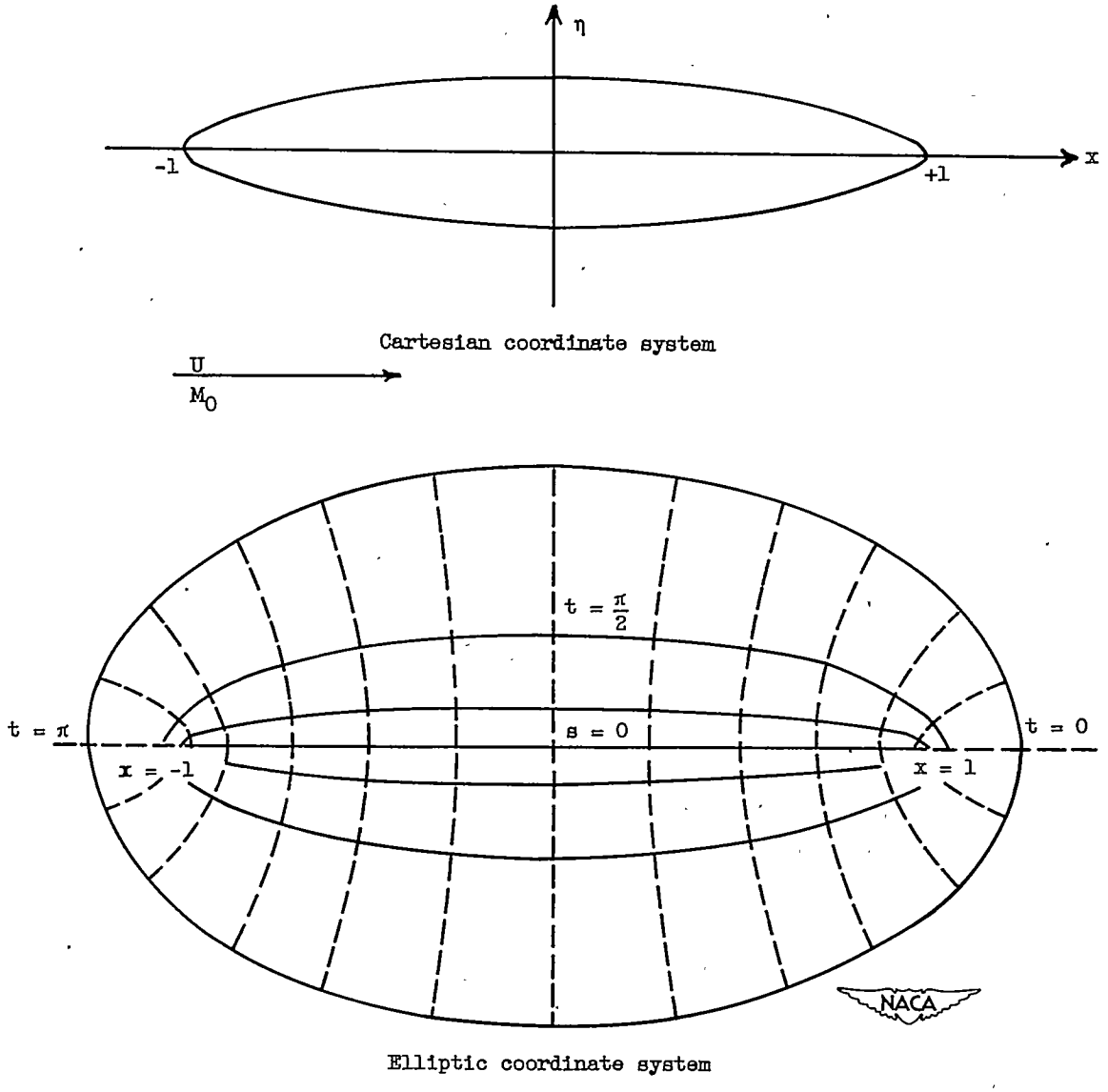

Figure 3. - Coordinate systems for two-dimensional body.

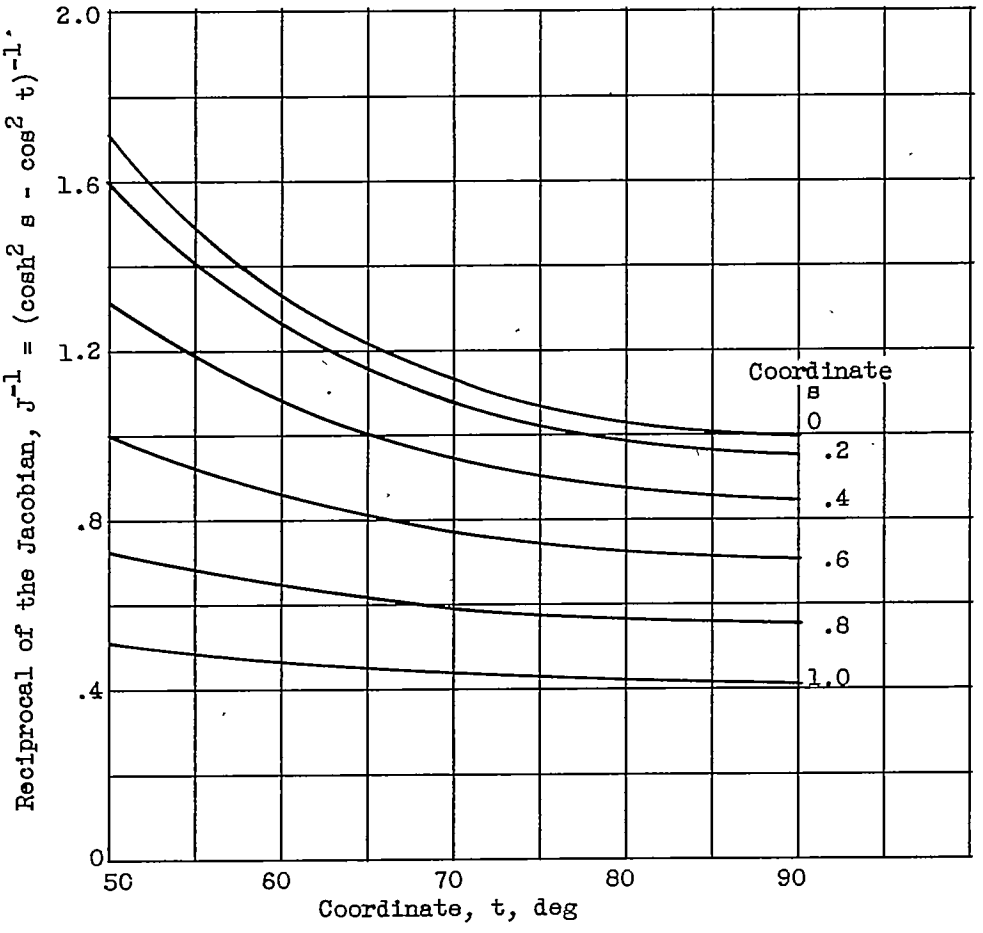

Figure 4. - Functional determinant of transformation $x = \cosh s \cos t$, $\eta = \sinh s \sin t$.

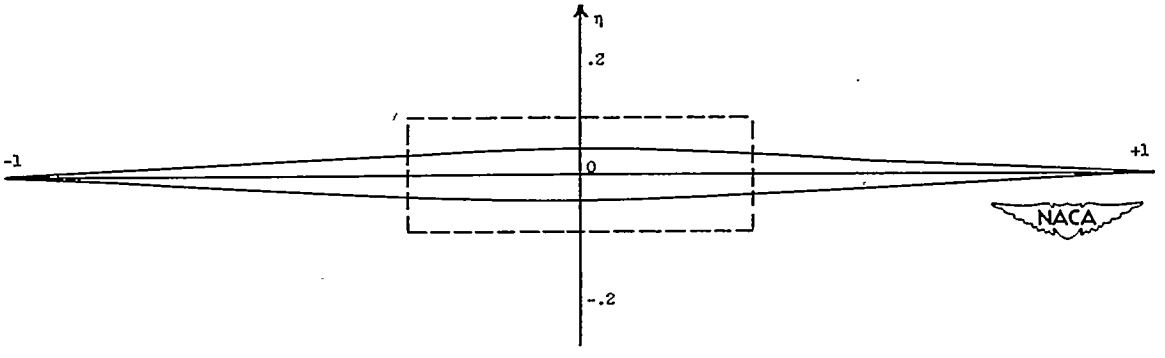

Figure 5. - Kaplan section and region of validity of simplified flow equation. Thickness ratio, 0.1; free-stream Mach number, 0.9.

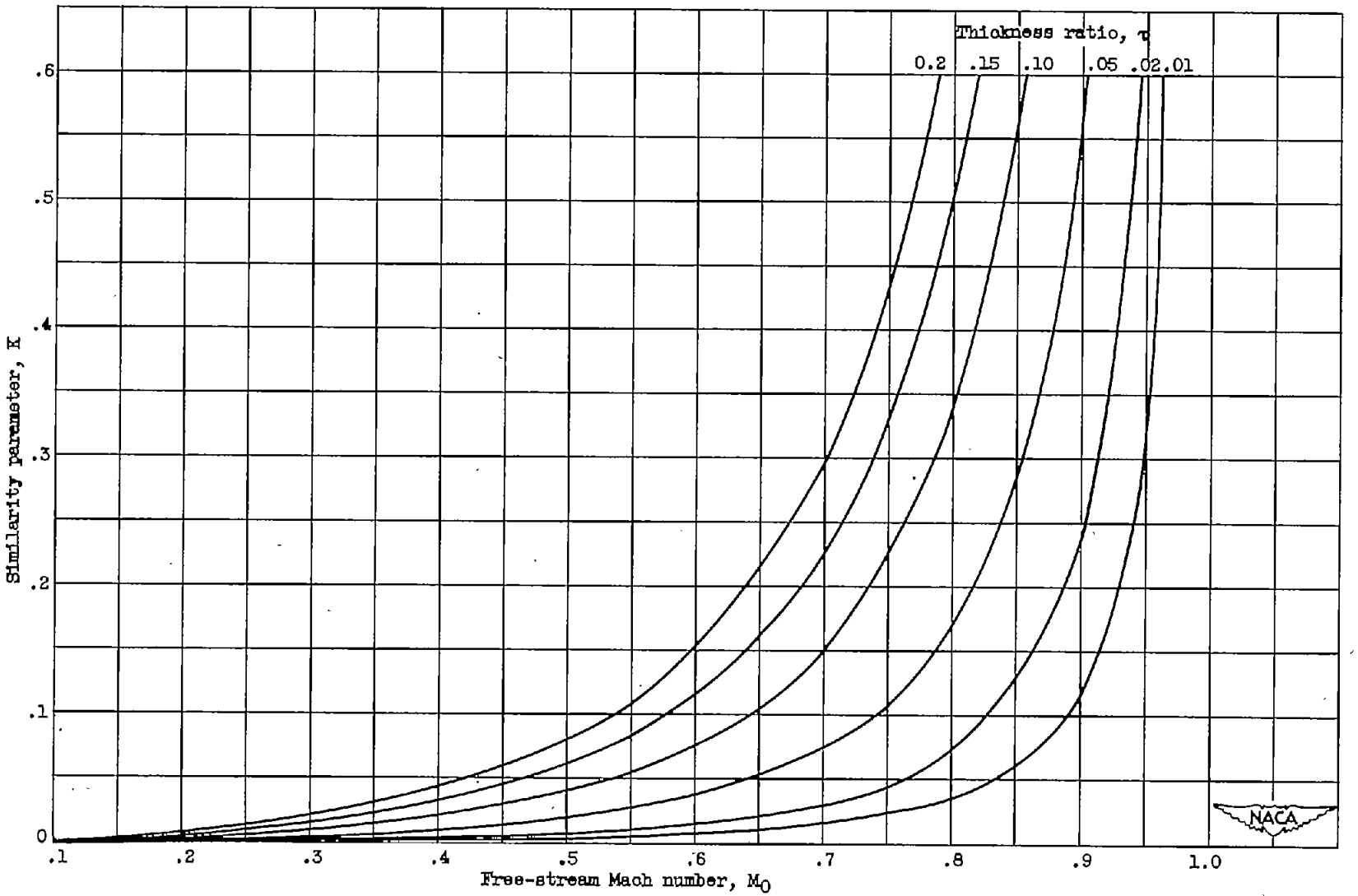

Figure 6. - Curves of similarity parameter against free-stream Mach number for several values of thickness ratio.

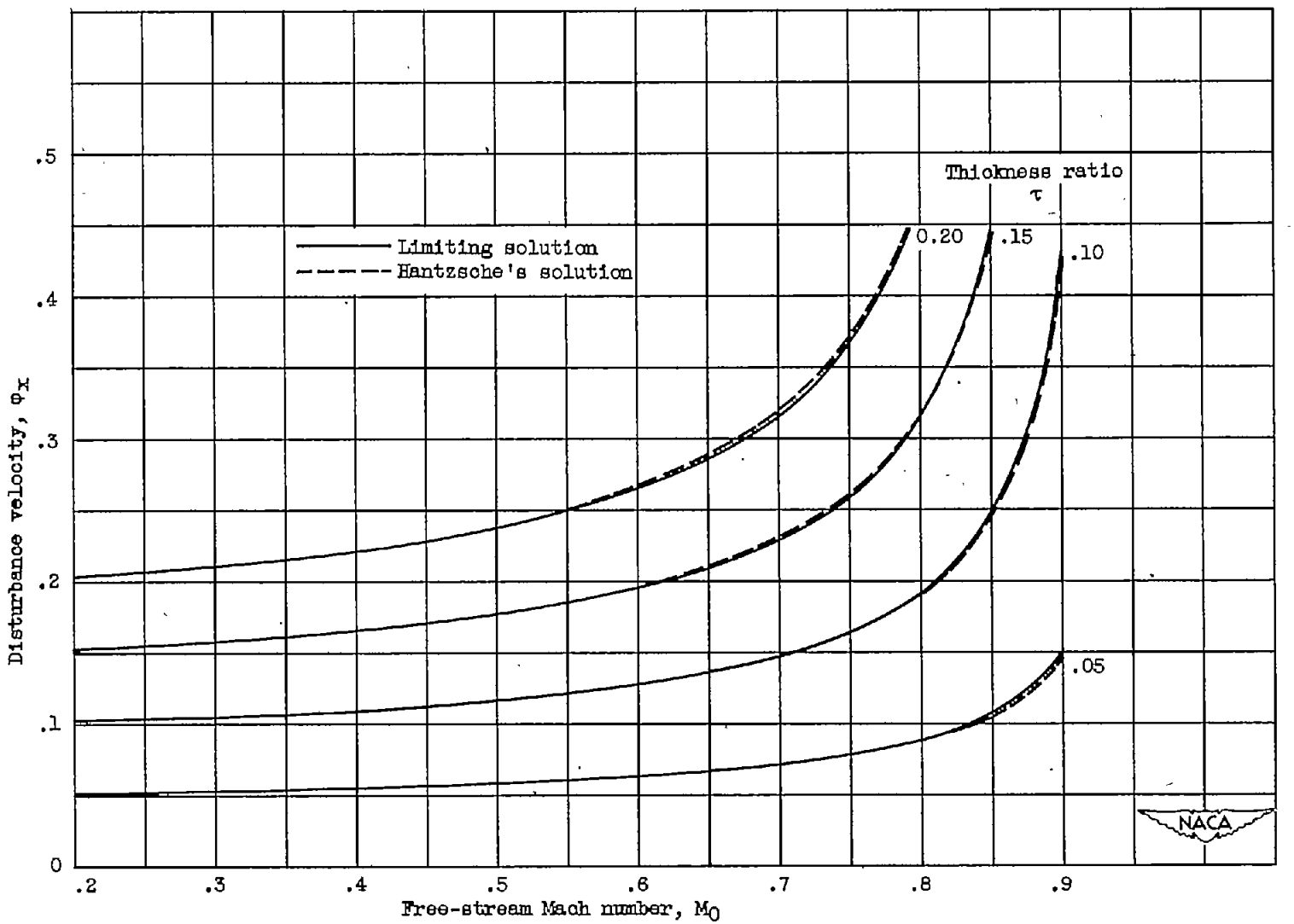

Figure 7. - Disturbance velocity at center of ellipse. Three approximations.

2275

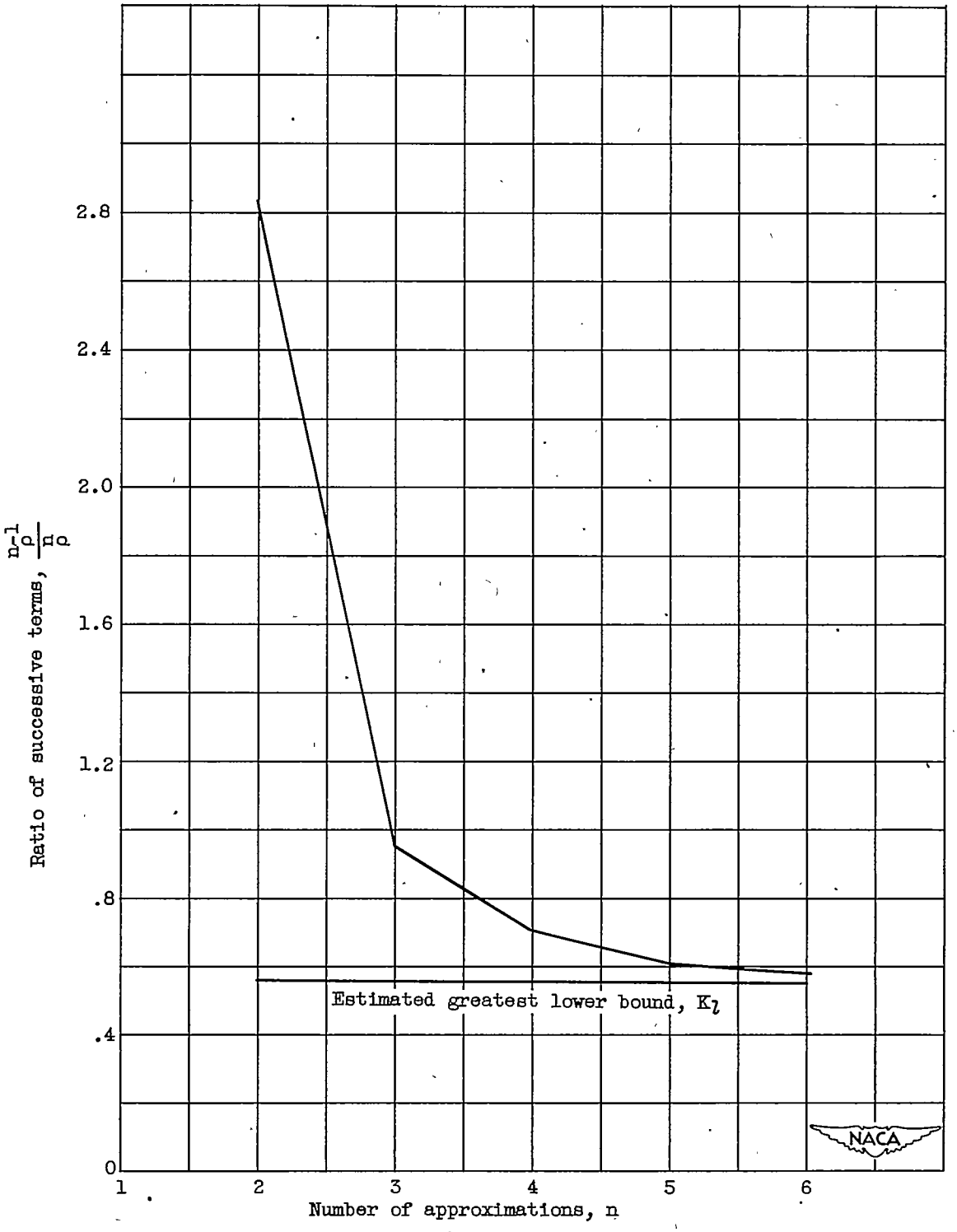

Figure 8. - Estimation of potential limit similarity parameter for elliptic cylinder.

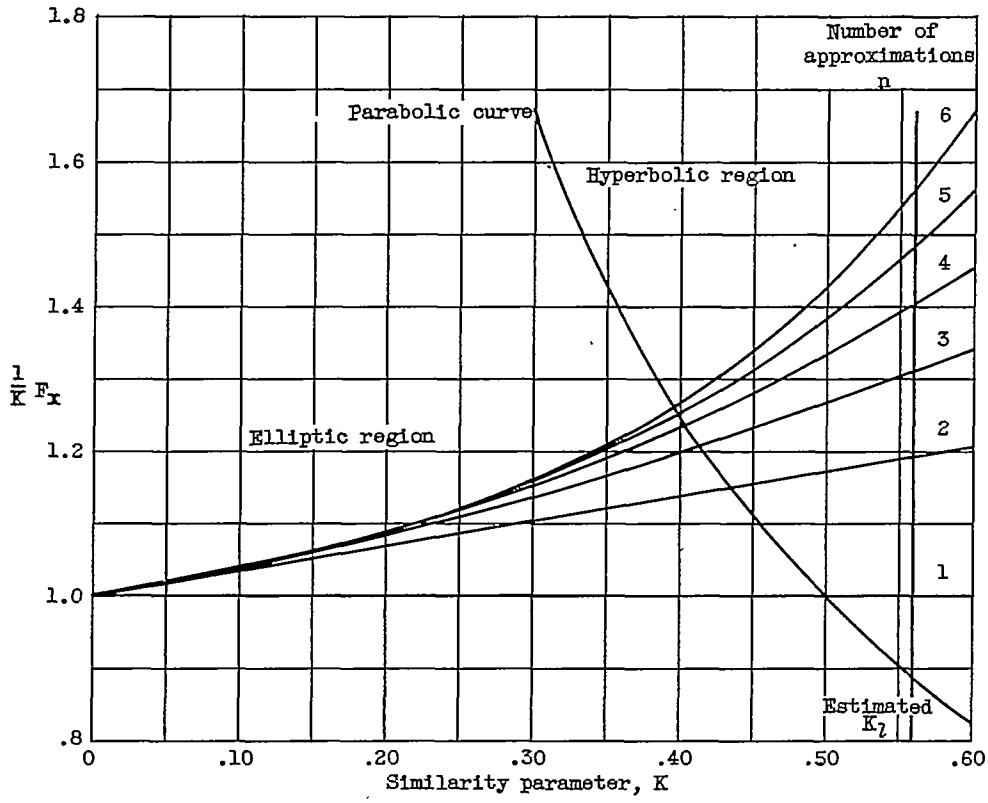

Figure 9. - Maximum velocity increment on surface of thin ellipse.

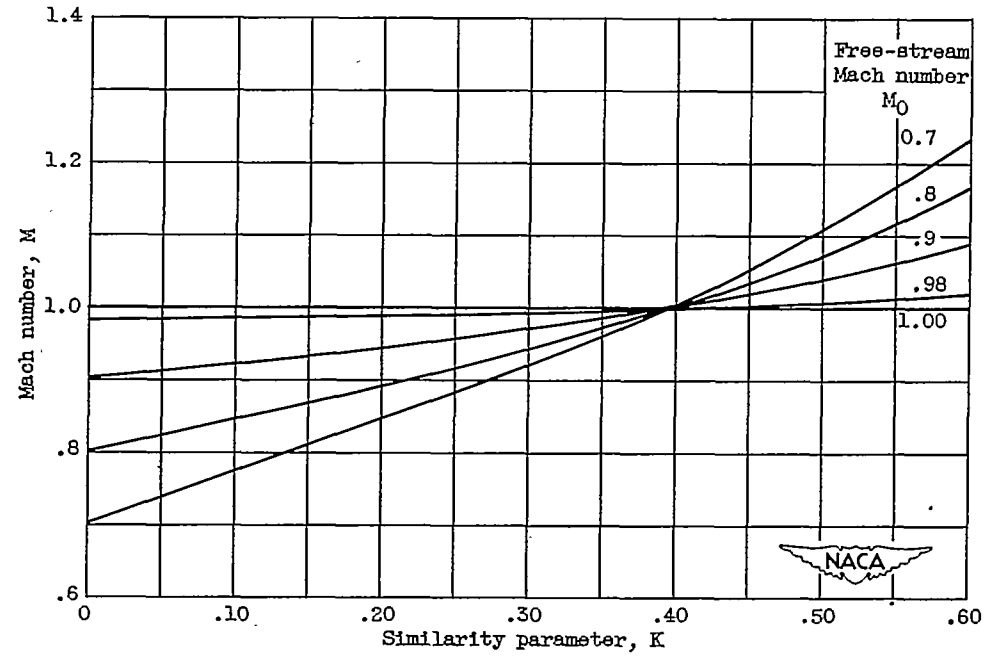

Figure 10. - Maximum local Mach number on surface of thin ellipse. Six approximations.

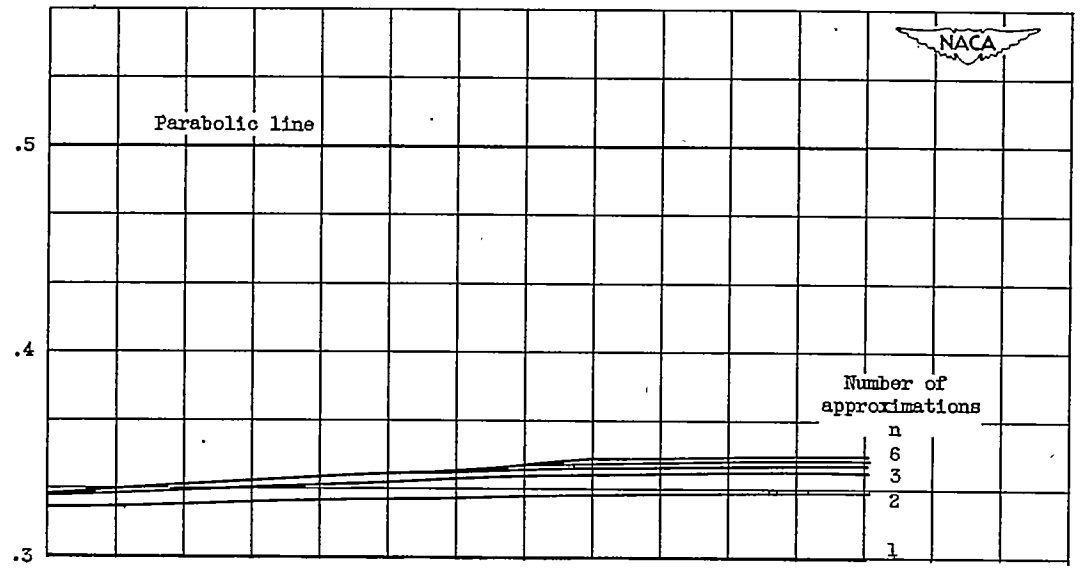

(a) Similarity parameter, 0.3.

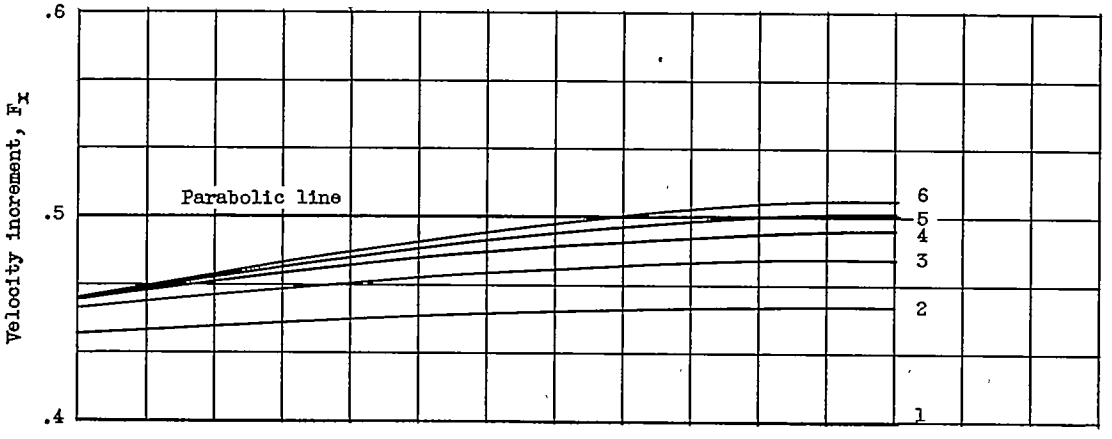

(b) Similarity parameter, 0.4.

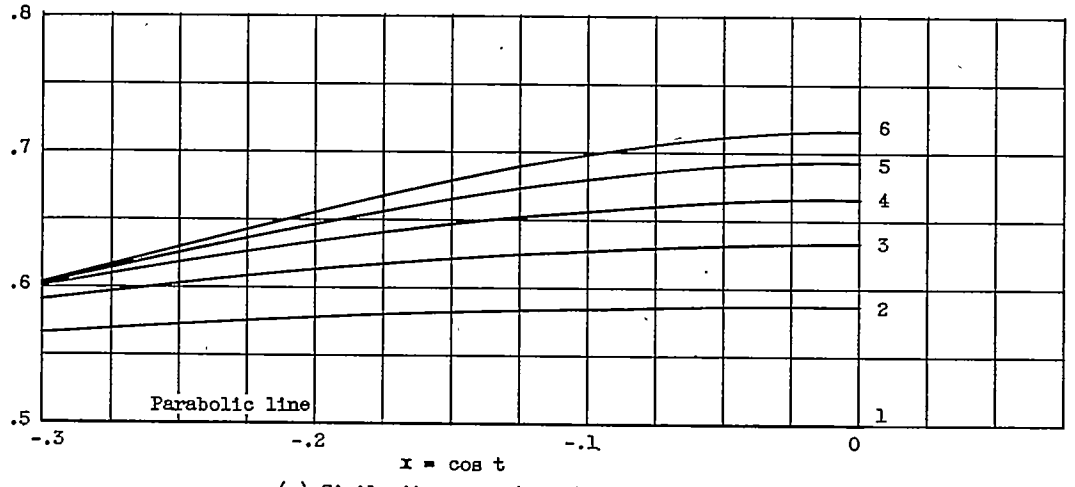

(c) Similarity parameter, 0.5.

Figure 11. - Velocity increment at surface of ellipse.

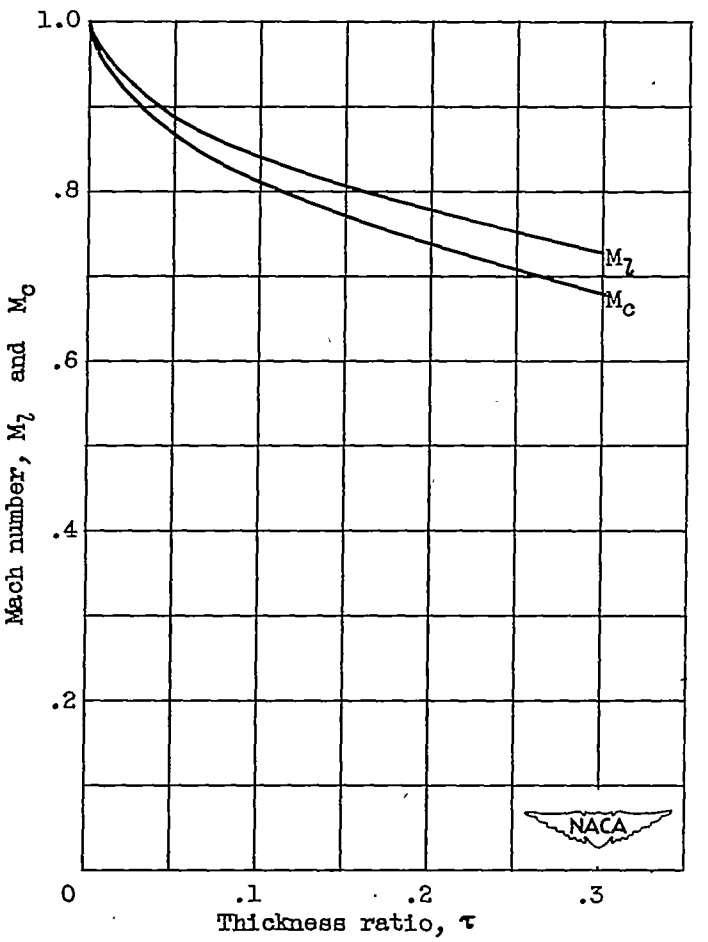

Figure 12. - Potential limit Mach number and critical Mach number for ellipse.

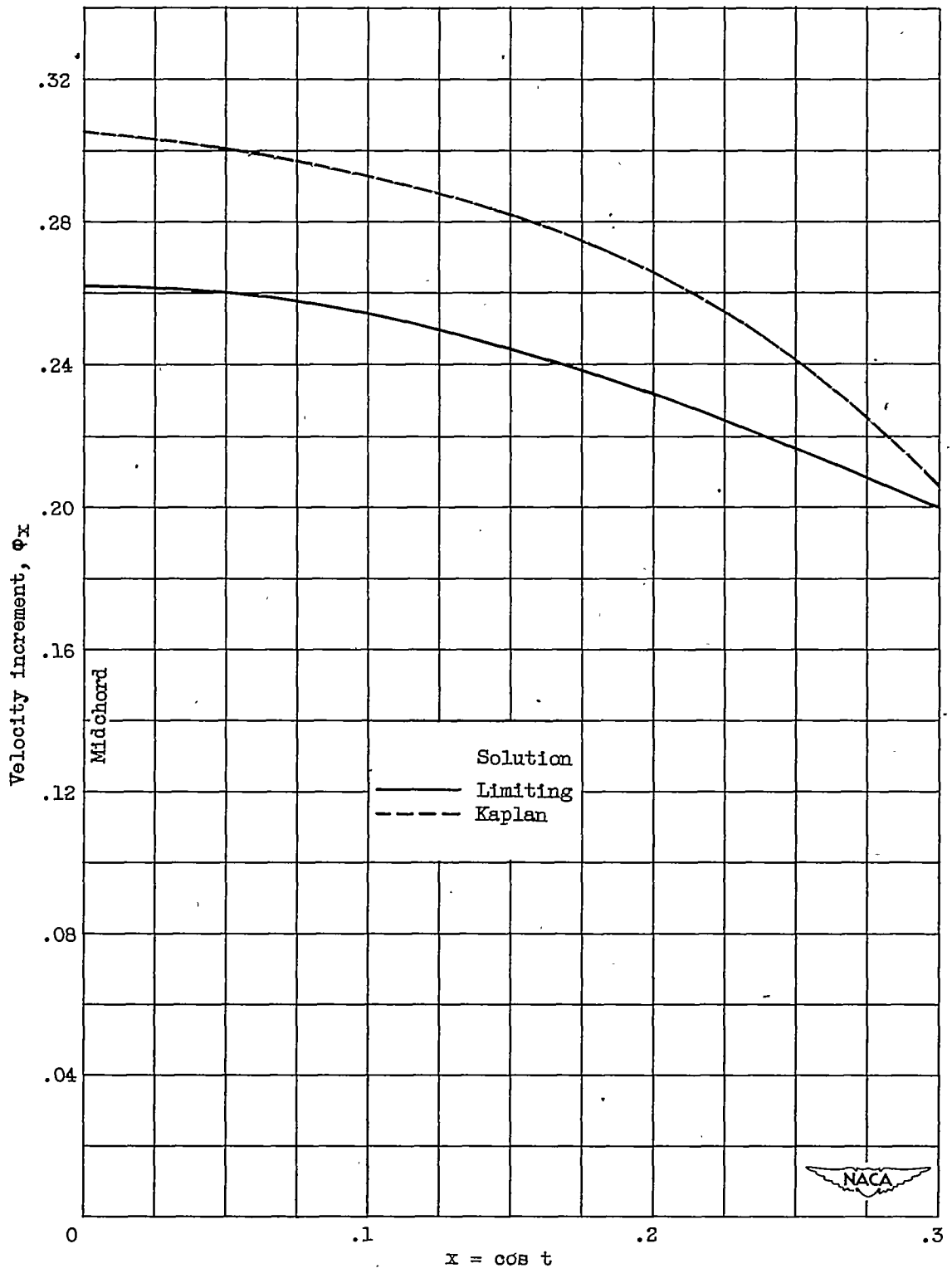

Figure 13. - Velocity increment on surface of Kaplan section. Thickness ratio, 0.10; free-stream Mach number, 0.75; three approximations.

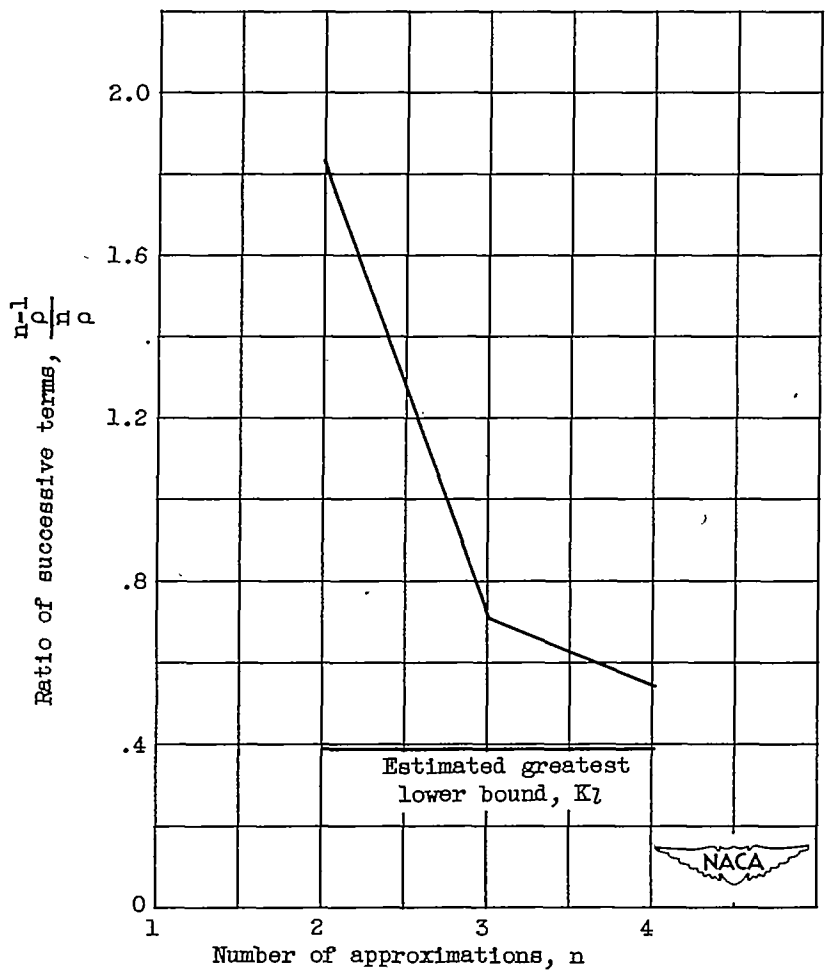

Figure 14. - Estimation of potential limit similarity parameter for Kaplan section.

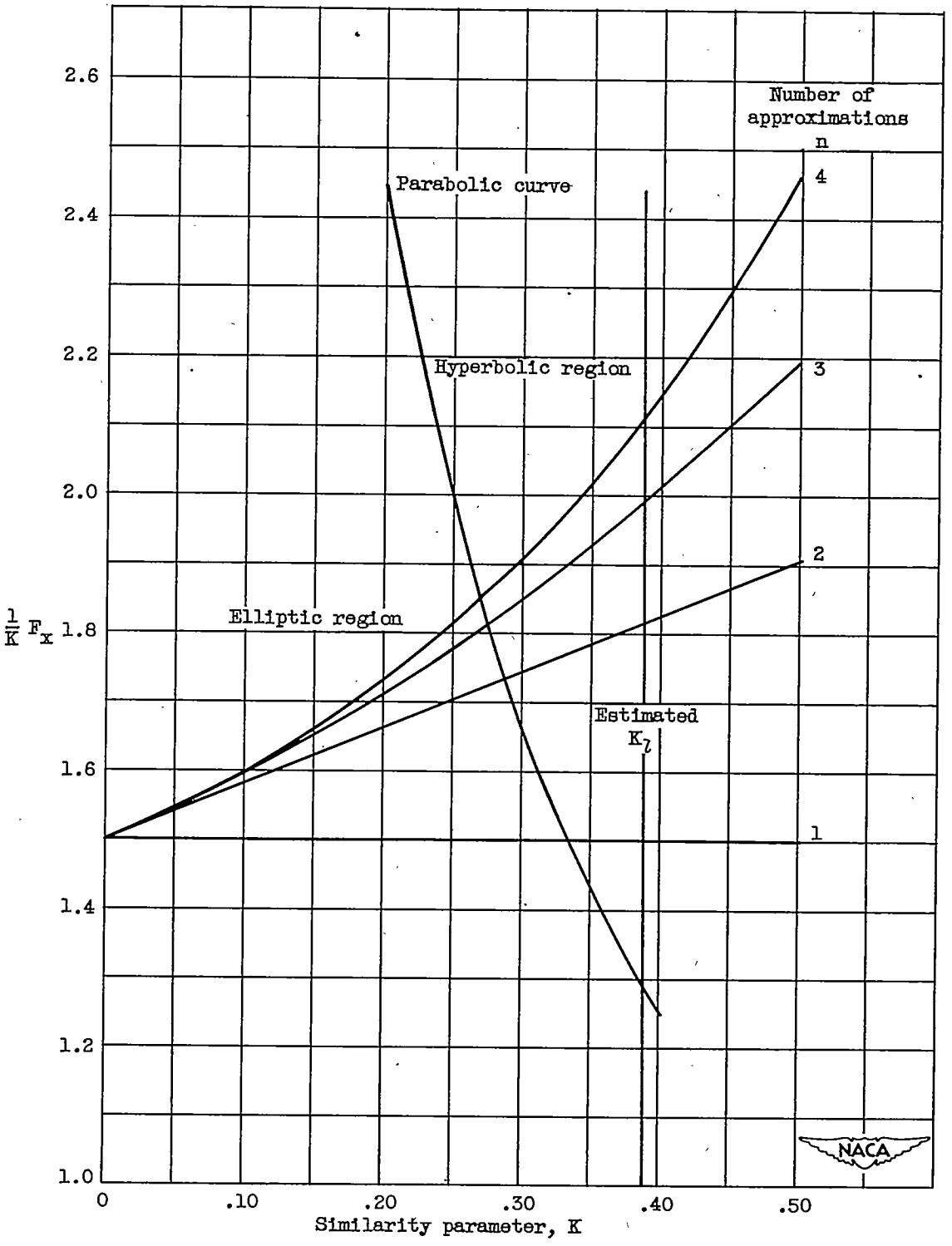

Figure 15. - Maximum velocity increment on surface of Kaplan section.

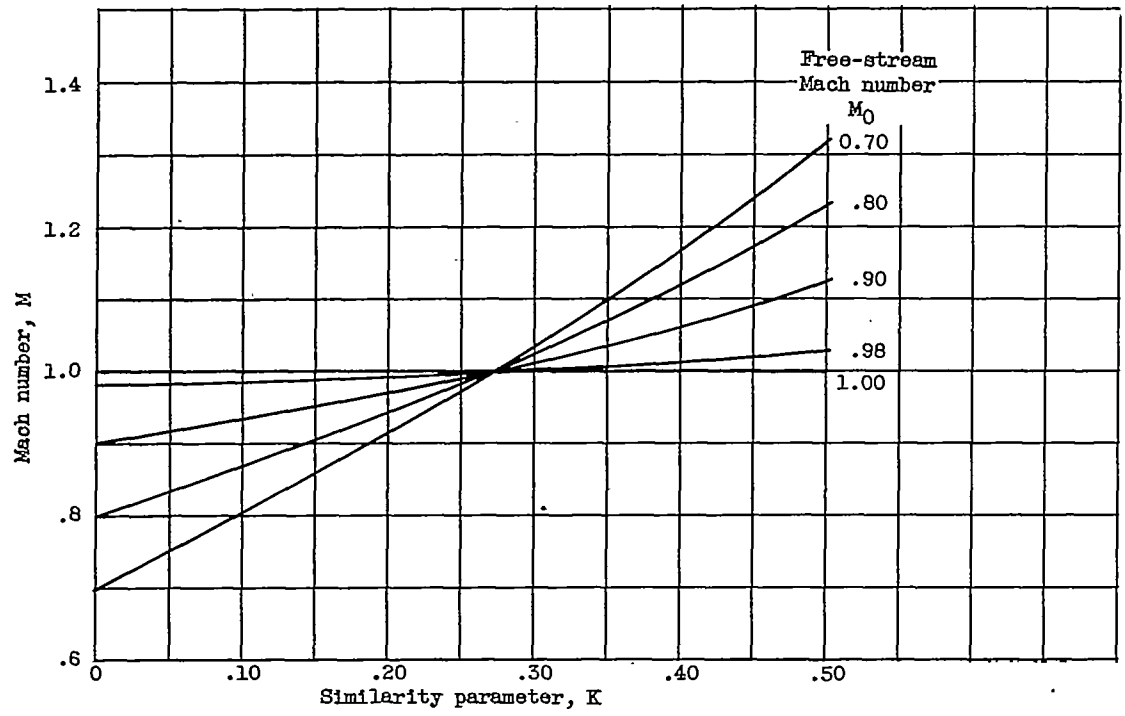

Figure 16. - Maximum local Mach number on surface of Kaplan section.

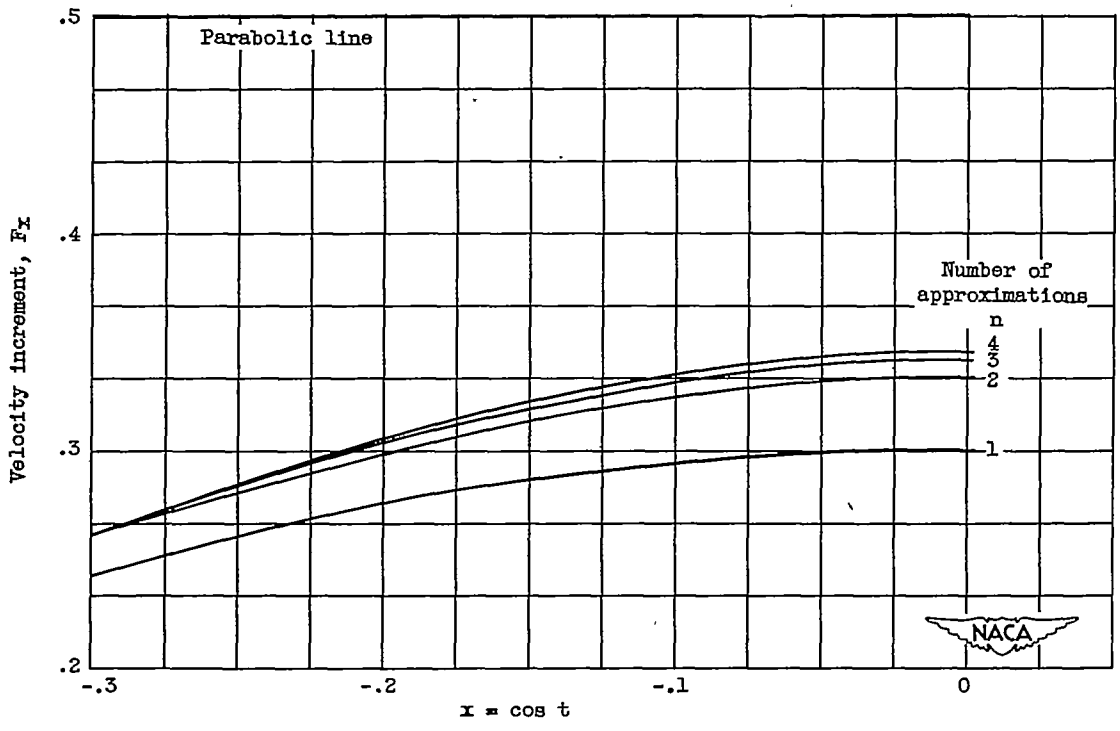

(a) Similarity parameter, 0.2.

Figure 17. - Velocity increment at surface of Kaplan section.

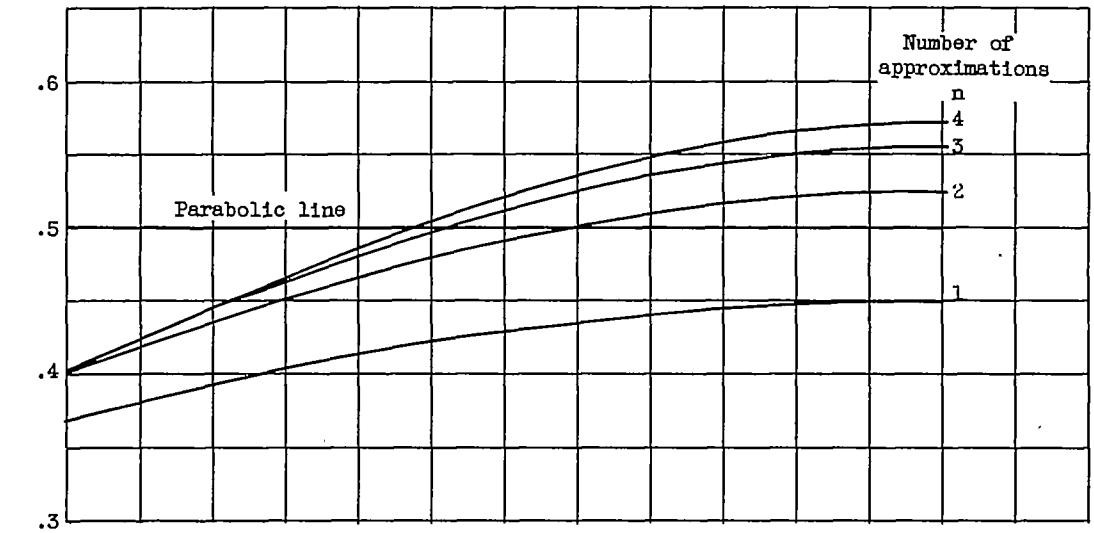

(b) Similarity parameter, 0.3.

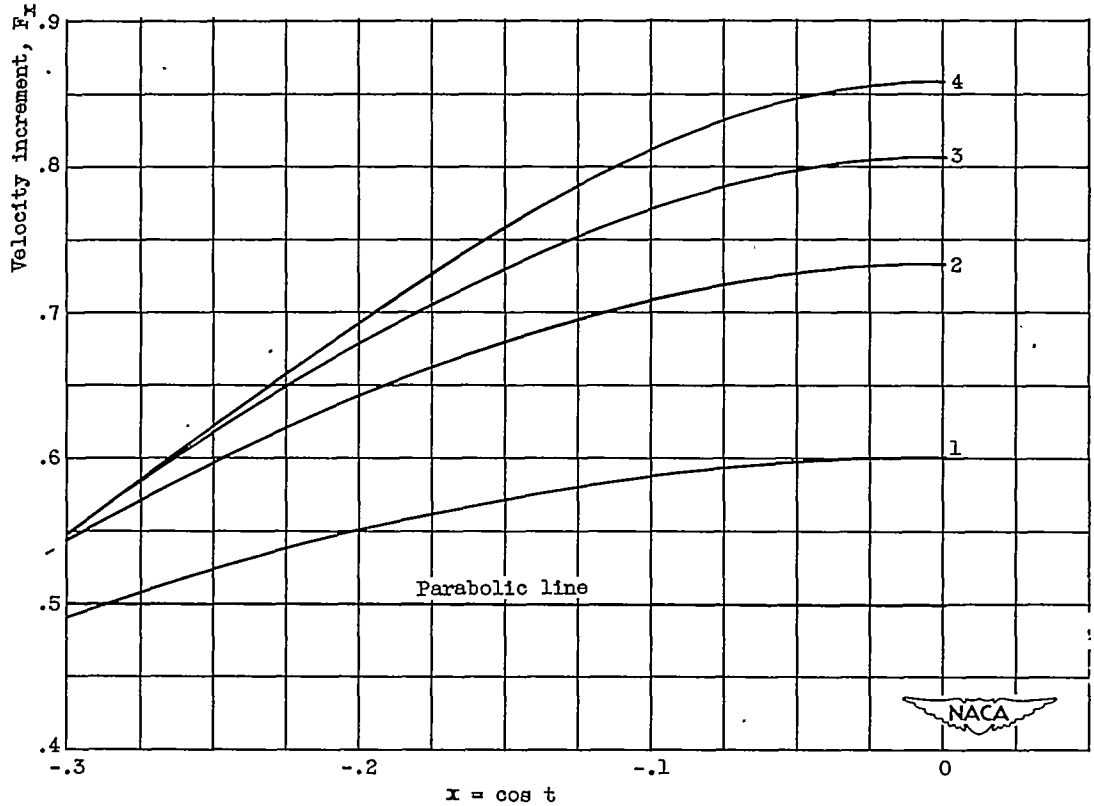

(c) Similarity parameter, 0.4.

Figure 17. - Concluded. Velocity increment at surface of Kaplan section.

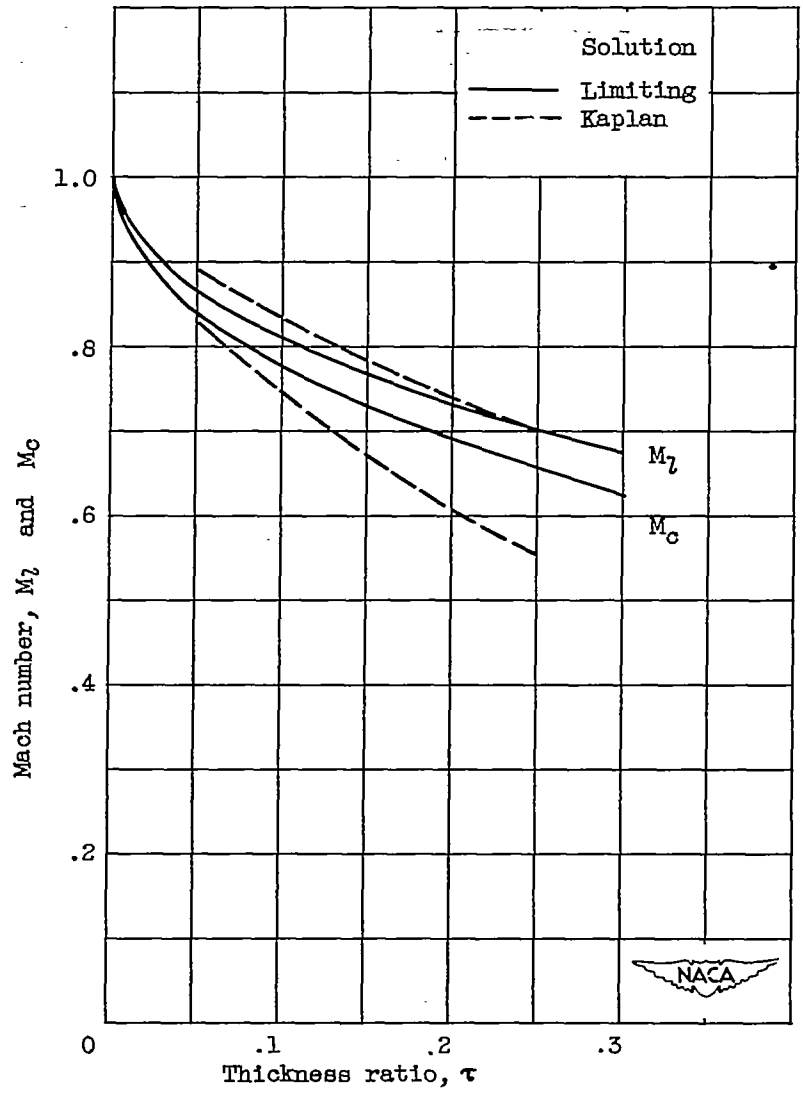

Figure 18. - Potential limit Mach number and critical Mach number for Kaplan section.

NACA-Langley - 10-17-51 - 1000